



**Politecnico
di Torino**



Politecnico di Torino
Master Degree course in Mechanical Engineering
Academic year 2023/2024
October 2024

Specifications and conceptual design of a mobile manipulator for the construction sector

Master Degree Thesis

Supervisor:
Alba Perez Gracia

Candidate:
Francesco Maggi

Abstract

This thesis investigates the design and application of a mobile robot aimed at automating the scanning and digitization of buildings at demolition sites using Ground Penetrating Radar (GPR). The objective is to enable the robot to autonomously navigate through complex building environments, such as corridors and around obstacles, while maintaining the capability to access nearly any point within a structure. The design integrates a robotic manipulator arm on a mobile base and necessary sensors to support comprehensive site analysis. The robot integrates a manipulator arm equipped with multiple sensors, including GPR, LiDAR, and depth cameras, to perform detailed scans that contribute to the creation of accurate Building Information Models (BIM). This study discusses in detail the robot's design considerations. By analyzing data collected from GPR and LiDAR sensors through advanced algorithms, the robot can identify material compositions, detect structural features, and optimize the demolition process by predicting material recovery and waste reduction opportunities. The result of this thesis presents a potential starting concept for the actual design of the robot, taking into account the actual or realistic dimensions of all the elements that will constitute the final robot.

Contents

1 INTRODUCTION	5
1.1 Motivation	5
1.2 Objectives	5
2 DISCOVER project	6
2.1 State of art	6
2.2 objectives	6
2.2.1 Main challenges	7
3 Specifications and components	8
3.1 Robot dimensions	8
3.2 GPR antenna	11
3.3 Robotic arm	15
3.3.1 UR20	19
3.3.2 Controller	24
3.4 Lifting column	26
3.4.1 Lifting column for cobot	29
3.4.2 Controller	31
3.5 LiDAR	33
3.6 Camera	37
3.7 Base	40
3.8 Logistic issues and considerations	43
4 Base kinematics and static stability	45
4.1 Statics	45
4.2 Base kinematics	47
5 Final design	50
5.1 Cilindric frame	51
5.2 External frame	51
5.3 Controller boxes	53
5.4 LiDAR	55
5.5 Cobot	56
5.6 Lifting column	59
5.7 Gpr and cameras	61
6 Conclusions	63

List of Figures

1	Corridor dimensions	9
2	Geometrical draw of a corridor	10
3	Max lenght of the robot	10
4	Exemplary GPR scheme	11
5	Scattering mechanism	12
6	Screening Eagle GP8800 GPR	13
7	Example of scansion with GP880	14
8	Different types of robotic arms	16
9	UR10e Cobot	17
10	UR10e payload curve	18
11	Height of UR10e in resting configuration	18
12	Differences in payload and reach between UR20 and UR10e cobots	20
13	UR20 Link 1 lenght	21
14	Height in rest configuration	22
15	Max height without lifting mechanism	22
16	OEM control box for UR10e	24
17	Control box dimension [mm]	25
18	Different types of lifting columns	26
20	Motor housing dimensions	27
19	DL11XL dimensions	27
21	Maximum velocity for 4 DL11 connected	28
22	ELEVATE lifting column for cobot from LINAK	29
23	CBD6S Control box	31
24	CBD6S draw	32
25	LiDAR functioning	33
26	Example of 3D point cloud	33
27	OUSTER OSDome LiDAR	35
29	OSDome draw	36
28	OSDome range precision and range accuracy	36
30	Working principle of structured and coded light camera	37
31	Working principle of stereo depth camera	38
32	RealSense Dept Camera D435i	39
33	Mobile base first concept	40
34	Cylindrical part of the mobile base with and without external frame	41
35	Center of mass in rest configuration	46
36	COM in maximum horizontal extension	47

37	Wheeled mobile robot scheme in bidimensional space	47
38	Example of omni wheels	48
39	Kinematic model of the robot	48
40	Chassis scheme	49
41	Full robot concept	50
42	Cilindric frame dimensions	51
43	Lower frame dimensions	52
44	External frame dimensions	52
45	Example of base support	52
46	Possible configuration of controllers	53
47	Example of pc box	54
48	Representation of LiDAR FOV	55
49	Cobot scanning the ground	56
50	Cobot distance from the edge of the base	57
52	Maximum extension touching the floor	57
51	Robot height in rest position	58
53	Max heigth without a lifting	58
54	Maximum reachable height	59
55	Lifting column in the base	59
56	Cobot center of mass	60
57	Camera and GPR mounted on the cobot	61

1 INTRODUCTION

1.1 Motivation

The construction activities in EU consume half of the 1800 million tonnes of materials extracted in Europe. The construction sector is also responsible for 39% of global greenhouse gas emissions [17]. Building materials and products are key components that impact embedded environmental footprint, energy efficiency, durability, and safety. A digital twin of buildings is needed to reduce construction and demolition waste and to safely manage hazardous materials. By having the data, it is also possible to identify the process for multi-cycle component management. A digital model would help expedite demolition planning and understand the building's key points of interest.

The development of a robot capable of automating the process currently performed partially by humans, which involves high resource and time expenditure, could pave the way for a future of significant savings and material reuse in the construction industry.

1.2 Objectives

The objective of this work is the design of a mobile robot. Its purpose is to work at demolition sites to scan buildings by means of a GPR antenna and obtain a BIM (building information model) from a distance. The robot must be able to move freely within the buildings, traversing doors, corridors and various obstacles, while still being able to reach almost anywhere in the structure. Therefore, it is necessary to understand the environment in which the robot operates and the challenges it may encounter, while endeavoring to propose realistic solutions. The technologies required by the robot must be explored, their functionality and compatibility understood, and their integration into the robot studied. Therefore, it is desired to find different solutions and select the one that, as of today, despite incomplete project information, may prove to be the most functional and feasible. For each device required for the project's implementation, we aim to explore viable options available in the sector market to understand whether they are already commercially available or if internal design and development within the department are necessary. According to the specifications of the devices being sought, the goal is to propose a viable design and determine functional possibilities and limitations.

2 DISCOVER project

2.1 State of art

The field of robotics in demolition is just beginning, with current advancements focusing on automated demolition and robots designed for sorting waste. There are also autonomous mobile robots that specialize in scanning building geometry and creating digital models [3]. Lee (2015) [18] introduced a system based on Building Information Modeling (BIM), where robots equipped with sensors can visually identify materials that can be reused.

Omnidirectional mobile manipulators (MMs) are a combination of omni mobile robots and manipulator arms, greatly enhancing their capabilities to operate over large areas and perform tasks that require physical contact [15].

Ground Penetrating Radar (GPR) technology has primarily been used manually for assessing buildings. However, automatic detection methods are being explored, such as identifying corrosion. Artificial Neural Networks (ANNs) have been trained using laboratory images to predict radar data based on factors like temperature, humidity, chloride levels, and the condition of rebar surfaces [27].

Identifying materials on-site involves a blend of expertise from demolition auditors or contractors, along with non-destructive testing methods and devices for measuring dimensions and thickness. Research has focused on automating the classification of building materials, utilizing techniques like LiDAR scanning for capturing material properties, surface geometry and roughness [24]. Various sensor technologies including GPR, LIBS, and UT are also being employed for material composition analysis and detecting hidden elements like reinforcement and cracks [8]. While there's progress in integrating data from multiple sensors, the interpretation of these measurements still heavily relies on human experts and manual analysis.

2.2 objectives

The project objectives are:

- To create a set of autonomous and synchronous robotics systems for the precise, fast and less labour-intensive analysis, identification and digitisation of materials and construction components from existing built works, based on mobile manipulators and new data fusion approaches
- To achieve fully automatic understanding of data coming from cameras, ground-penetrating radar (GPR), laser-induced breakdown spectroscopy (LIBS), etc. using sensor fusion techniques and machine learning algorithms, rapidly analysing the properties and char-

acteristics of elements and materials

2.2.1 Main challenges

The main challenge is the fully autonomous navigation in the variable conditions of demolition sites, while mapping with the desired precision, and the accurate interaction with the elements for invasive testing are all challenging operations. The online identification of materials and elements is currently done only at the visible, surface level, and with the help of human verification. The dynamic modification of the navigation according to the findings is not solved in the state of the art. Finally, the communication between robots and with the BIM needs to provide feedback on when the identification of geometry, materials and elements is accurate enough.

The application of AI methods segmentation and classification of construction materials, including hidden elements, is an active research topic, in which robustness and repeatability are the main challenges. The great variability of shapes, grades and compositions is a challenge for classification algorithms and automatic pattern recognition based on indirect measurements. The main challenges include increasing the accuracy by reducing the uncertainty by combining different NDT methodologies and some invasive tests. The combination of autonomous invasive and non-invasive techniques also presents many challenges regarding communications, localization and action self-assessment. Moreover, the decision about where the invasive measurements are needed can be also determined by the automatic analysis of data from GPR, LiDAR and other techniques.

3 Specifications and components

3.1 Robot dimensions

First step for robot design is to understand the useful space for maneuverability. The robot will have applications in both civil and industrial buildings. The project aims for general use in the states of the European Union, but these have different regulations for construction. It is important to note that most of the buildings to be demolished date back to the first half of the 20th century, a time when there was no general regulation for buildings in most of Europe. An Example is Portugal, where the first General Building Regulation for construction, health, safety and aesthetics was approved in 1951 [11]. There are many other national construction standards that add up to regional regulations. All this leads to building regulations being fragmented and complex [22].

The minimum dimensions not to be exceeded are those of standard doors. Most used ones for indoor are $70 - 73 \text{ cm}$ but in many situations, like for the bathrooms, doors of $60 - 63 \text{ cm}$ are used. No standard door is lower than 2 m . For this reason the maximum dimensions considered for the robot are $60 \times 200 \text{ cm}$.

In civil buildings it is difficult to find regulations indicating a maximum height, usually the minimum height of about 2.40 m is stated. More complete information can be found for example in the Spanish law of 1969 [14] shown in the table.

Considering also more recent laws limiting the maximum height of a ceiling between 2.90 m , 3 m was taken as the reference for this project taking into account the existence of special cases.

In industrial environments there are generally more spacious passageways and openings. More challenging here is to reach the high ceilings of $4 - 5 \text{ m}$ that can be found. The solution to remedy this problem would be to scan ceilings that are too high through the floor of the upper floor or roof (if walkable), in the case of the top floor. For this, the target height of 3 m is maintained, while taking into account possible difficulties in industrial environments.

The maximum length of the robot is more uncertain as a measurement because there must

	Minimum [m]	Minimum [m]	Maximum [m]	Maximum [m]
	Ground floor	Other floors	Ground floor	Other floors
Rural environment	2.50	2.40	3.00	2.80
Urban environment	2.80	2.50	3.60	3.00

Table 1: Floor height in Spain, law of 1969

be enough room to maneuver despite the fact that the robot can move in any direction. In the absence of firm data for the problems outlined above, older architectural drawing standards, in this case from Spain, were considered [13].

As shown in the figure 1 the minimum size is 90 *cm* but in case of columns or recesses it is possible to go up to 80 *cm*.

Distribuidor o pasillo - D

Superficie mínima

No se fija.

Dimensiones críticas

Según gráfico.

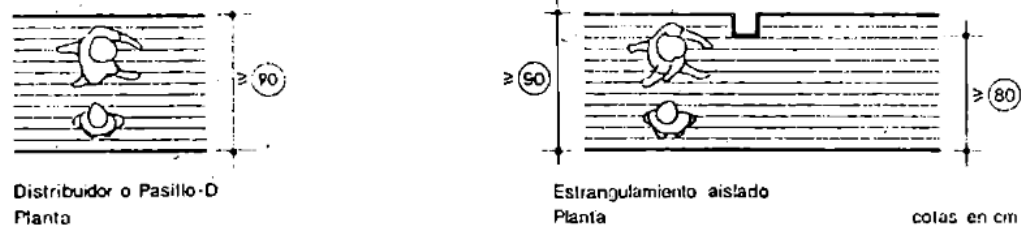


Figure 1: Corridor dimensions

[13]

Based on a well-known mathematical problem of a tube going around an angle [12]. Based on the figure 2, having the corridor width c the demonstration leads to equation 1

$$\tan^3(\theta) = 1 \quad (1)$$

and thus to the result 2

$$\theta = 45^\circ \quad (2)$$

A maximum length of about 106 *cm* was estimated as shown in the figure 3.

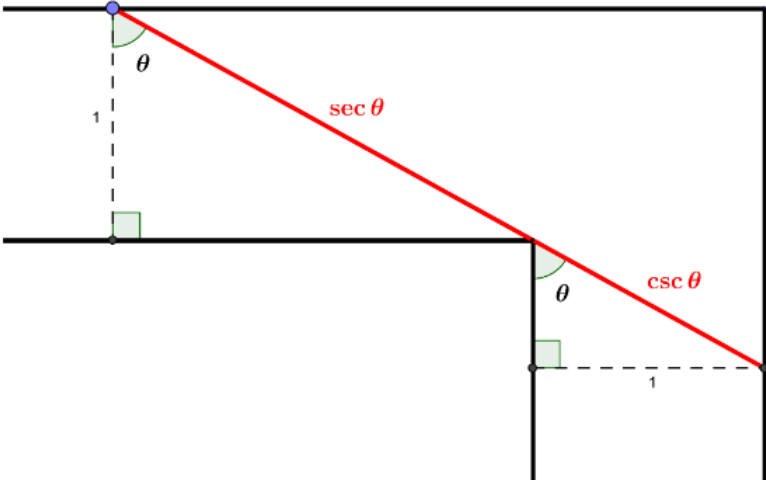


Figure 2: Geometrical draw of a corridor

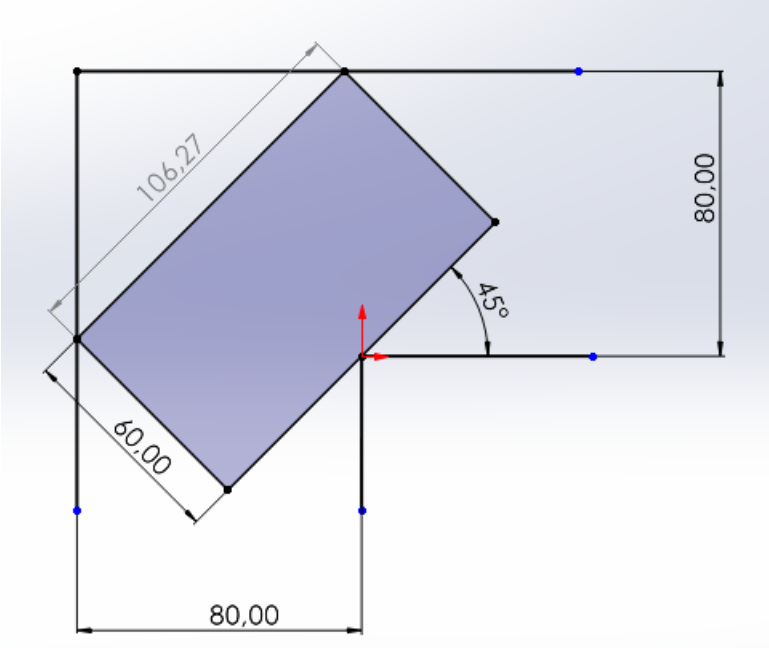


Figure 3: Max lenght of the robot

3.2 GPR antenna

Ground Penetrating Radar (GPR) is a non-invasive geophysical technique that utilizes radar pulses to visualize underground structures. Due to its capacity to deliver detailed and high-resolution data about subsurface structures without the need for excavation, GPR has become a crucial tool in various fields, such as geology [6], archaeology [16], engineering [5], and environmental science. The practical application of Ground Penetrating Radar (GPR) involves

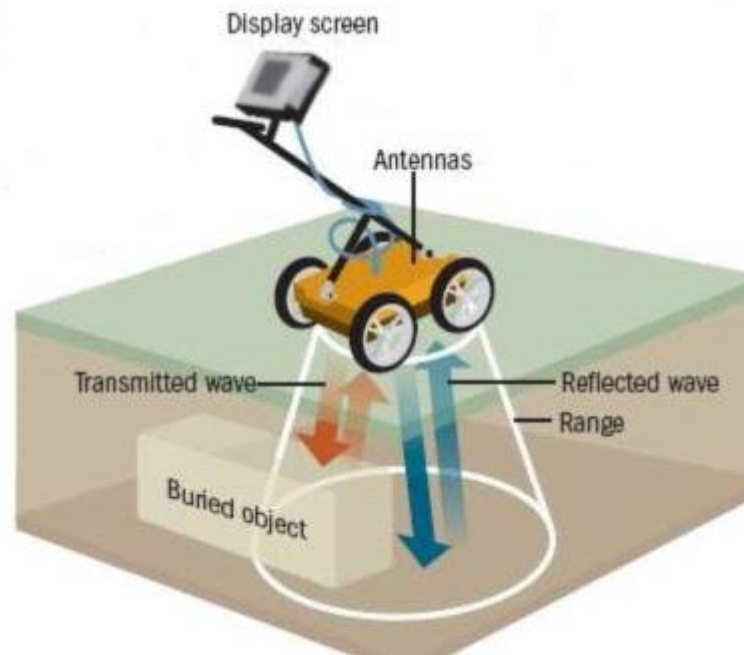


Figure 4: Exemplary GPR scheme

emitting high-frequency electromagnetic waves from a transmitting antenna into the ground. These waves travel through the material at a speed primarily determined by the material's permittivity. As the wave propagates downward, it spreads out until it encounters an object with different electrical properties. The wave is then scattered from the object, with portions being reflected back to the surface and detected by a receiving antenna. This detected wave is recorded for later analysis.

GPR antennas function as transducers, converting electric currents into electromagnetic waves and vice versa. The design of these antennas aims to control and direct the radiation effectively. The transmitted waves' speed is influenced by the material's permittivity, forming the basis for using GPR to investigate subsurface structures. The time it takes for the wave to travel from the transmit antenna to the receive antenna is termed "travel time," measured in nanoseconds.

When a wavefront encounters an object with a different permittivity, scattering occurs. This scattering can take various forms: specular reflection, diffraction, resonant scattering, and re-

fraction (fig. 5). These phenomena are utilized to interpret the GPR data and identify subsurface features.

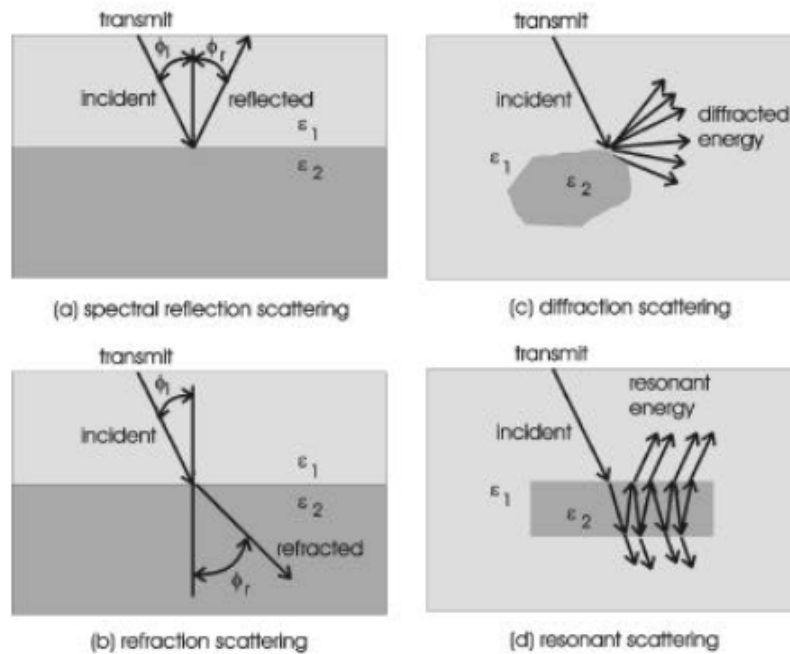


Figure 5: Scattering mechanism

GPR measurements can be conducted by moving the antennas continuously over the ground or at discrete points along the surface. Continuous mode allows for rapid data acquisition, while discrete mode offers flexibility. Combining both modes can provide an optimal balance of data quality and efficiency [10].

In today's market, there are GPR devices that are extremely compact and lightweight. The model selected for this project is the **GP8800** from *Screening Eagle*.



Figure 6: Screening Eagle GP8800 GPR

Its main applications are: areas close to walls and underneath pipes, irregular and curved surfaces and Concrete Quality Assessment. The main specifications are:

Measurement modes	Superline scan (1000 <i>m</i>) Area Scan (with Flexible Grid up to 100 <i>m</i> ²)
Radar technology	Stepped-frequency continuous-wave (SFCW) GPR
Modulated frequency range	400 – 6000 <i>MHz</i>
Penetration depth	65 <i>cm</i>
Battery	Flight-save, ,removable pack, 4xAA
Dimensions	89 × 89 × 76 <i>mm</i>
Weight	487 <i>g</i>
Depth accuracy	±5 <i>mm</i>
Accuracy in distance	< 2%
Minimum distance between objects	3 <i>cm</i>
Connection	WiFi and USB-C to display unit
Maximum linear speed	1 <i>m/s</i>

Table 2: GP8800 main specifications

It is also equipped with a wireless wheel and a USB-C connection for connecting a powerbank or, as in our case, an external battery. Small dimensions allow great versatility to scan any critical point near walls or narrow spaces.

The extremely low weight relative to the payload of the manipulator (3.3), on the other hand,

allows for maximum mobility without having to worry about having to reduce speed due to power limits or excessive inertia of the end effector.

This model of GPR does not need a control box but simply connects the device to a PC or any screen thanks to WiFi or USB to get real-time images of the scan. This reduces the space needed for controllers on the external frame. In addition, the company has developed a dedicated app that is extremely easy and intuitive to use.

In addition, the company offers the possibility of mounting the device on a telescopic rod, which allows the device to reach the ceiling in a normal house from a person standing on the floor, so having no problems with the offset of the payload as shown in the figure 10, it can easily be mounted to the flange of the cobot to reach greater distances.

The device, as can be seen in the figure 6, is equipped with a small side wheel that can be mounted on each side and allows the antenna to operate only when it is moving along a wall. It is also essential to indicate the axis of the scanning direction.



Figure 7: Example of scansion with GP880

3.3 Robotic arm

A robotic arm is a device constructed of linkages connected by appropriate joints so that it may move in space and with the degrees of freedom needed for the task at hand. Frequently, the robotic manipulator may be trained to do specific tasks. It is additionally referred to as anthropomorphic because of how close in function it is to a human hand.

A robotic arm is composed of:

Base: is the foundation of the robot affected by the weight of all other components.

Joint: are articulation points along the robotic arm where movement occurs. Depending on the design, robotic arms may feature various types of joints, such as revolute (rotational), prismatic (linear), or spherical (multi-axis), allowing for a wide range of motion.

Links: are the segments that connect the joints of a robotic arm. Typically constructed from metal or composite materials, these rigid structures provide structural integrity and transmit forces and motion between the joints.

Actuators: are the components that generate motion in a robotic arm. Depending on the application requirements, actuators can be electric, pneumatic, hydraulic, or piezoelectric. They convert energy into mechanical motion, enabling the robotic arm to move its joints and perform tasks.

End Effector: is a tool or attachment mounted at the robotic arm's end to perform a specific task

Sensors: they provide feedback to the control system of the robotic arm, enabling it to sense and adapt to its environment.

Control system: is the brain of the robotic arm, responsible for coordinating the movements of the actuators based on input commands and sensory feedback. It ensures the robotic arm operates safely, accurately, and efficiently while performing its intended tasks.

There are several types of robotic arms. They differ primarily in their structure and applications. Articulated arms, resembling a human arm with six degrees of freedom, are used in manufacturing and assembly. SCARA robots, with fast and precise horizontal movements, are ideal for pick-and-place and packaging tasks. Delta robots, featuring a three-arm structure, excel in speed and precision for sorting and assembly. Cartesian robots, which move along orthogonal axes, offer rigidity and precision for CNC machining and 3D printing. Cylindrical robots operate within a cylindrical volume, suitable for assembly and spot welding, while spherical robots, utilizing spherical coordinates, are useful in complex spaces. Cobots, designed to work safely

alongside humans, are employed in small-scale assembly, inspection, and medical procedures. Finally, hybrid robots combine features from different types for complex tasks requiring precision and flexibility.

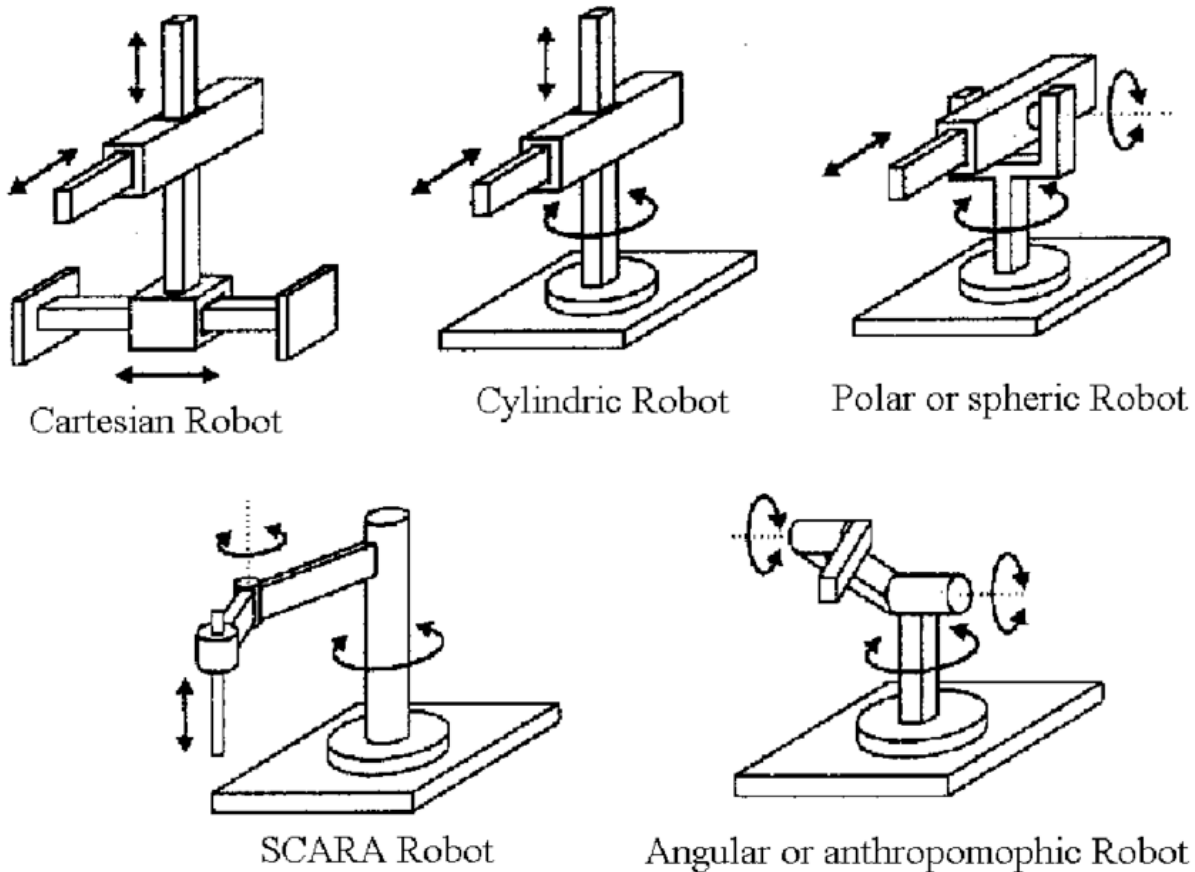


Figure 8: Different types of robotic arms

Together with the moving base, the manipulator is the main part of the robot. Its function is to support and move the GPR to enable scanning of the walls as well as the ceiling and floor. It is necessary that it be very flexible and long enough to reach the points of interest, at the same time, however, it cannot exceed the size limits given in 3.1. Furthermore, a certain level of safety is required by having people who might work around the robot. These reasons led to the choice of a cobot.

Cobots are Collaborative robots which have several advantages:

- Cost-effective
- Safe for humans

- Lightweight and space saving
- Flexible to deploy
- Easy programming
- Fast setup
- Flexible automation

For simplicity of development, a commercial manipulator model was sought.

Universal Robot stands out for reliability and ease of use as one of the leaders in the cobot sector. The **UR10e** model has been chosen for his flexibility given by the 6 joints with a $\pm 360^\circ$ working range each and a limited footprint. The robot's size allows easy navigation even in tight spaces, and its light weight does not allow the robot to be more stable.

Since the height in the rest configuration with the first link perpendicular to the ground is about 850 mm as seen in the figure 11, the base can have a more flexible height being far from the limit stated in chapter 3.1. The maximum speeds and torques of the joints are listed in the table 4 [2].



Figure 9: UR10e Cobot

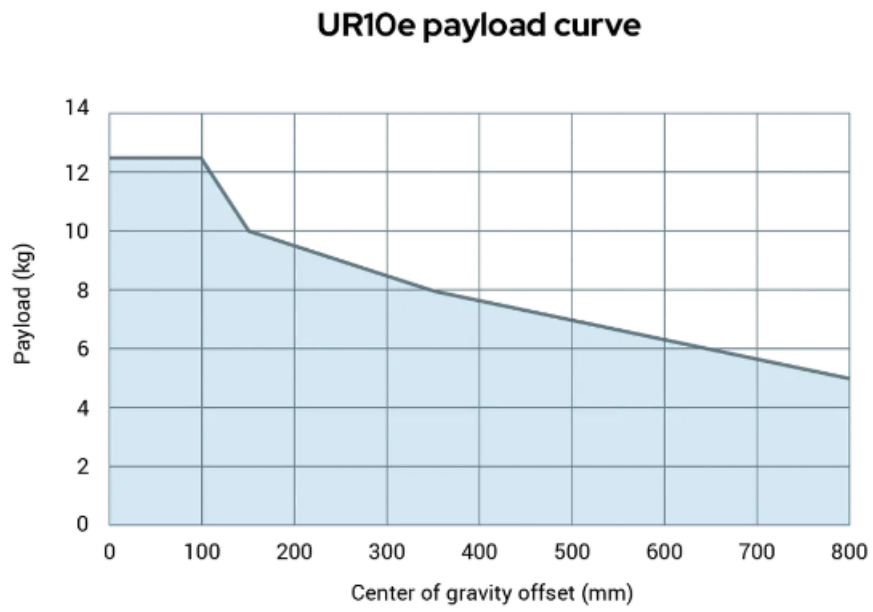


Figure 10: UR10e payload curve

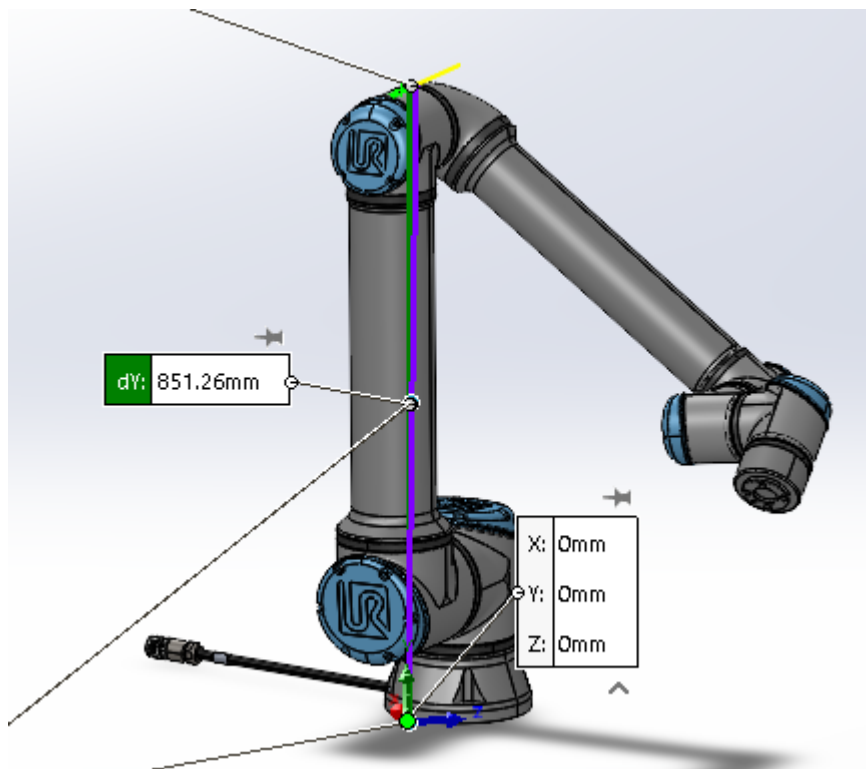


Figure 11: Height of UR10e in resting configuration

Payload in the entire workspace	12.5 <i>kg</i>
Reach	1300 <i>mm</i>
Degrees of freedom	6 rotating joints
Working range	± 360 for every joint
Footprint	190 <i>mm</i>
Materials	Aluminum, plastic, steel
Weight including cable	33.5 <i>kg</i>
Typical Tool center point (TCP) speed	1 <i>m/s</i>
Maximum power	615 <i>W</i>
Moderate operating settings	350 <i>W</i>

Table 3: UR10e main specifications

Joint	Max torque	Max speed
Base	330 <i>Nm</i>	120°/s
Shoulder	330 <i>Nm</i>	120°/s
Elbow	150 <i>Nm</i>	180°/s
Wrist 1	56 <i>Nm</i>	180°/s
Wrist 2	56 <i>Nm</i>	180°/s
Wrist 3	56 <i>Nm</i>	180°/s

Table 4: UR10e max velocities and torques

3.3.1 UR20

Instead of the UR10e cobot, the larger UR20 model has been considered. This is a more recent model from Universal Robots, featuring the specifications listed in the table 5.

Table 5: UR20 main specifications

Payload in the entire workspace	20 kg
Reach	1750 mm
Degrees of freedom	6 rotating joints
Footprint	245 mm
Materials	Aluminum, plastic, steel
Weight including cable	64 kg
Typical Tool center point (TCP) speed	2 m/s

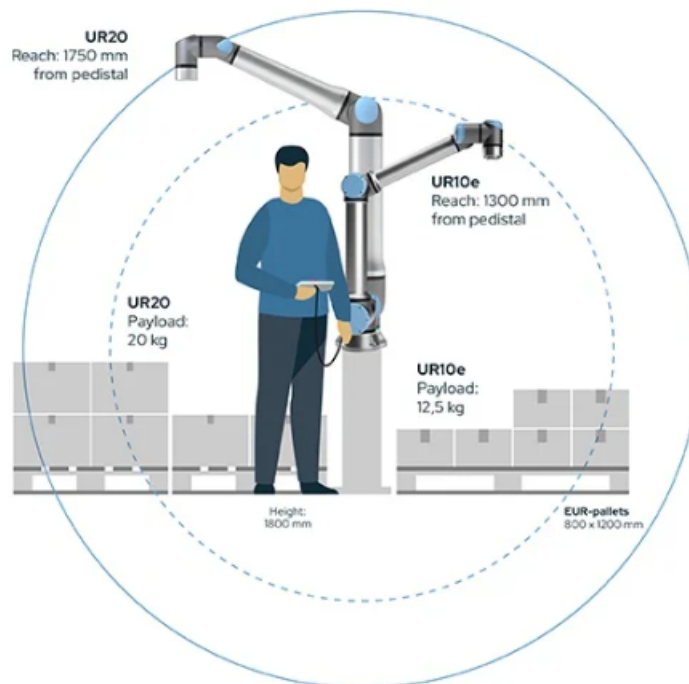


Figure 12: Differences in payload and reach between UR20 and UR10e cobots

As shown in the figure 13, there is sufficient space on the base to mount this robot, and it allows for reaching a good height without elevating movements. While an elevation system might still be necessary, it would only be modest in extent for residential buildings. However, compared to the chosen model, it is heavier and has significantly more inertia, which would require greater attention to the dynamic behavior of the entire robot to avoid unwanted tipping. The longer links also result in less versatility of movement, particularly in tight spaces where it might hit the walls. Specifically, Link 1 (between the shoulder and elbow joints) is about 1 m long (fig. 13), making scans problematic in scenarios where maintaining such a distance from the walls is not possible. Since link 1 has these dimensions, the base should also have a limited height (800 mm more or less as shown in fig. 15) to allow the overall height of the robot to be less

UR20 vs UR10e

Advantages	Disadvantages
Longer arm	Heavier
Reduced use of elevation systems	Prominent inertia
Greater overall reachable height	Limited base height
	Difficulty moving in confined spaces

Table 6: UR20 pros and cons

than 2 m as stated in chapter 3.1. This aspect is limiting for the development of the whole base and for the inclusion of the electronic part. It would be more difficult to assume to include the manipulator control box inside the mobile base and this would lead to less movement space for the first arm joint. In the figures 14 and 15 the total base height is 0.8 m .

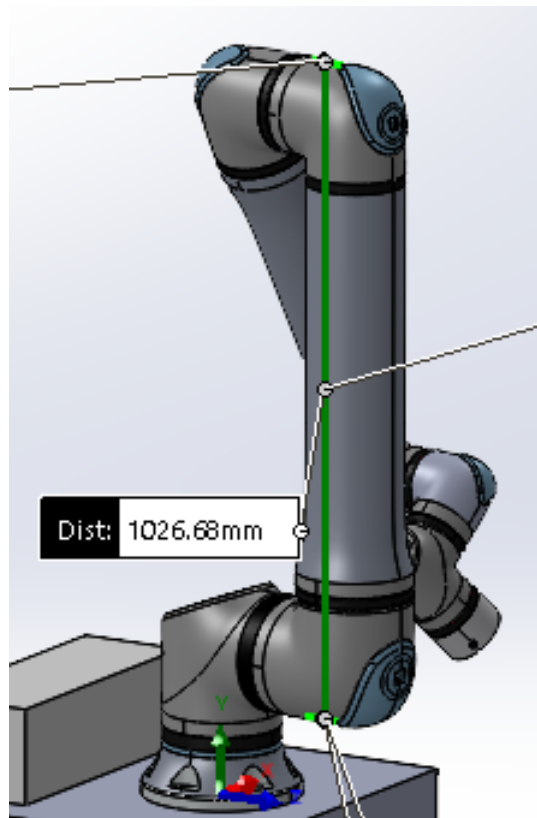


Figure 13: UR20 Link 1 length

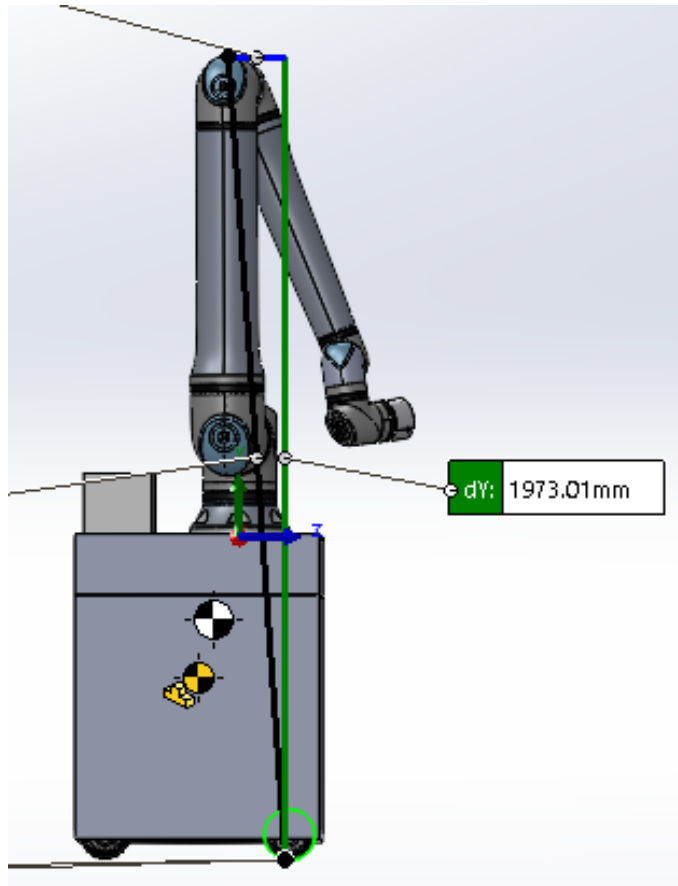


Figure 14: Height in rest configuration

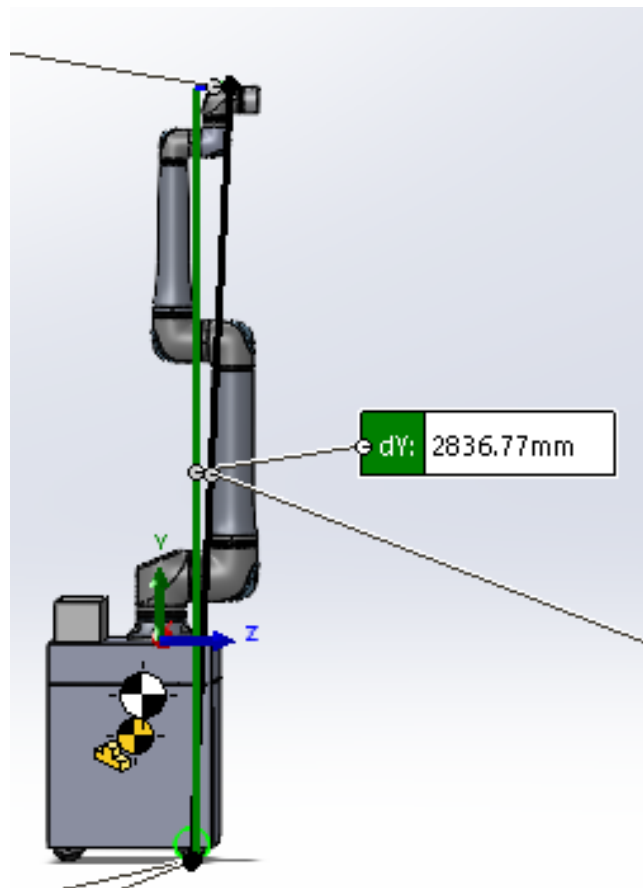


Figure 15: Max height without lifting mechanism

As can be seen in the figure 15, the maximum attainable height (approx. 2.84 m) is in any case not satisfactory for the design specifications, so even in this solution an elevation mechanism would be necessary. In this case, however, a smaller stroke would be required, which would make the movement quicker, more stable and less cumbersome in the base. For these reasons it is not considered among the advantages or disadvantages but depends very much on the final configuration of the mobile base.

3.3.2 Controller

Its controller must also be placed on the mobile base together with the manipulator. The **OEM 5.2** model was chosen, which compared to the standard model has smaller dimensions and lighter weight.



Figure 16: OEM control box for UR10e

Robot types	UR3e, UR5e, UR10e, UR16e
Operating temperature range	0 – 50°C
Control box size (W x H x D)	451 × 168 × 150 mm
Weight	4.7 Kg

Table 7: OEM 5.2 control box main specifications

Dimension are shown in figure 17.

Copyright ©2019-2024 by Universal Robots A/S. All rights reserved.

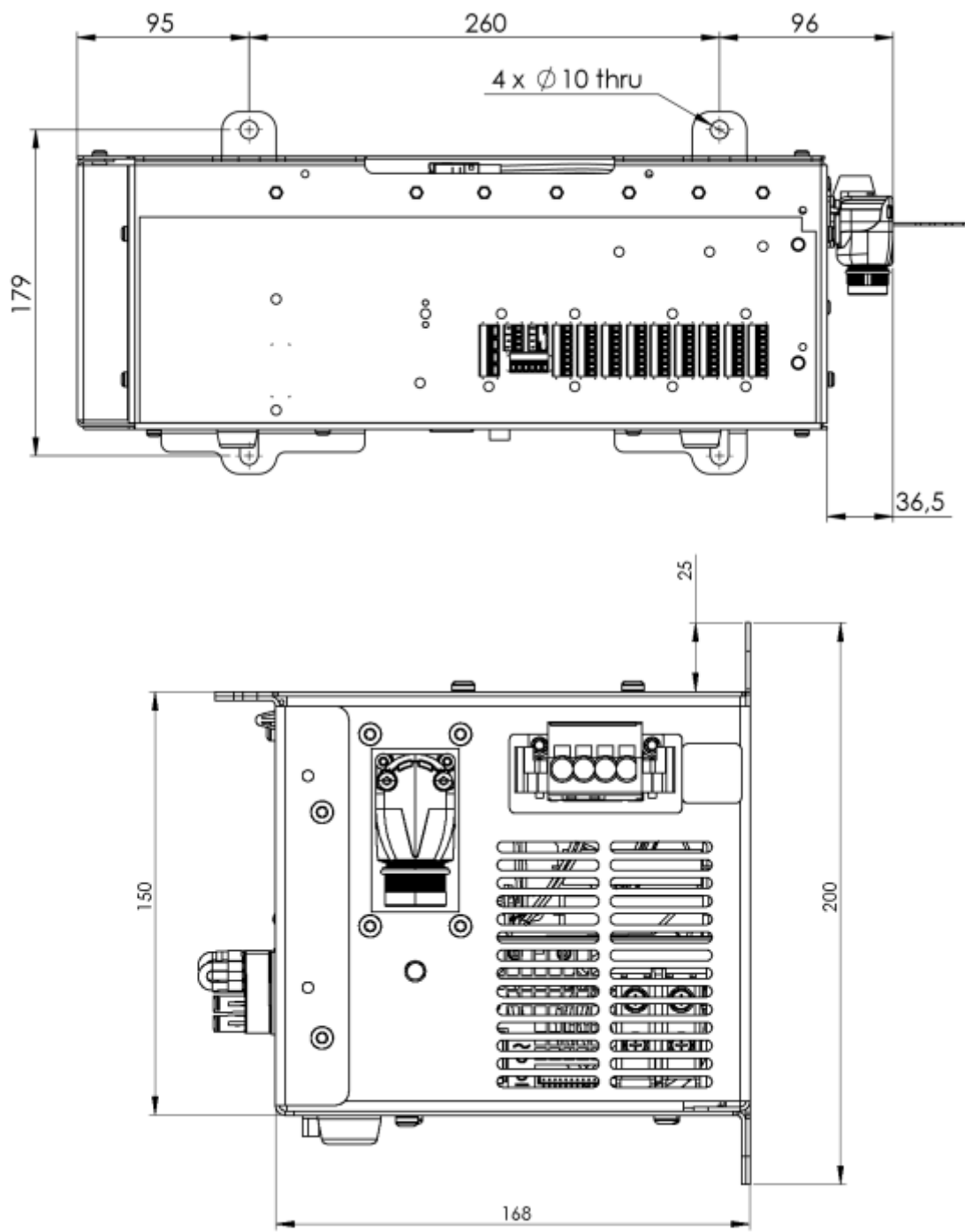


Figure 17: Control box dimension [mm]

3.4 Lifting column

Having limits on the maximum height would make it impossible to reach the ceiling in most civil and especially industrial buildings. For this reason the solution adopted is a lifting columns system.

Lifting columns, also referred to as telescopic pillars or actuators, offer an efficient solution for incorporating a lifting function into industrial equipment. Lifting column are electric linear actuators that allows the manipulator to achieve greater vertical extension maintaining a limited footprint and flexibility. These devices are quiet, robust and powerful.



Figure 18: Different types of lifting columns

Thanks to the telescopic structure, they can be mounted in the robot without changing the initial dimensions of the base, but allow a clear increase in the operating area of the robotic arm.

The choice for this project is the **DL11XL** model from *LINAK* (fig. 19).

The DL11 is a round three-part inline column, designed for desk application. The DL11 has reinforced column and optimised motor housing design for extra strength and stability. Its profile

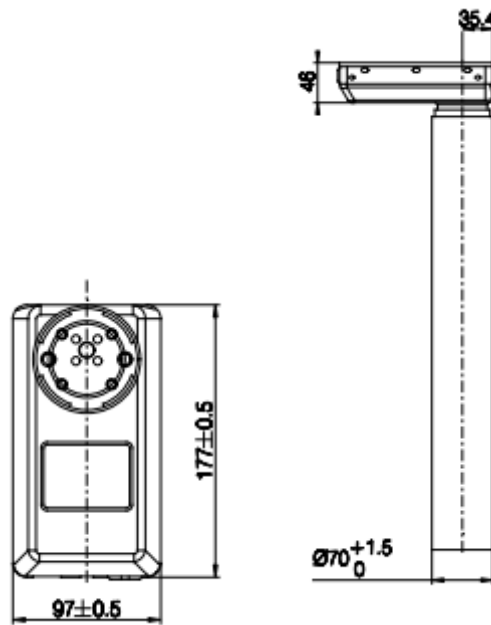
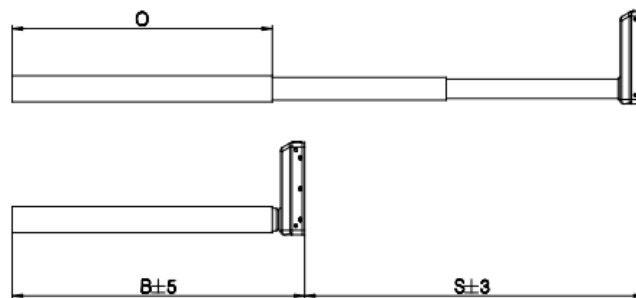


Figure 20: Motor housing dimensions

is secured against rotation/twisting. The system is operated by a DESKLINE control box (CBD), which ensures optimal parallel drive and maintains a pleasantly low noise level. The DL11 can be used as a single column or in systems with 2, 3, or 4 columns in parallel. The XL model offers the longest stroke in the series.



Version	Combination code	B (Built-in length) [mm]	S (Stroke length) [mm]	O (Outer profile length) [mm]
Standard columns				
EU	DL11xxxx0635575	575	635	498
PIEZO	DL11xxxxE650560	560	650	498
BIFMA	DL11xxxxxx665518	518	665	456
XL	DL11xxxxxx965740	740	965	663

Figure 19: DL11XL dimensions

Max. load	600 <i>N</i> per column
Max. speed	38 <i>mm/s</i> unloaded
Installation dimension	740 <i>mm</i>
Stroke length	965 <i>mm</i>
Bending moment	max 100 <i>Nm</i> dynamic
Weight	approx. 7.5 <i>kg</i> per column
Column dimensions	70 <i>mm</i> (outer profile)
Dimension motor housing	177 × 97 × 46 <i>mm</i>

Table 8: DL11XL main specifications

As shown in Chapter 5, 4 columns are used at the base vertices and the figure 21 shows the handling speed in this configuration. The curve apply to a centrally placed load. With moment load there will be increased friction in the columns, which will reduce the lifting force correspondingly.

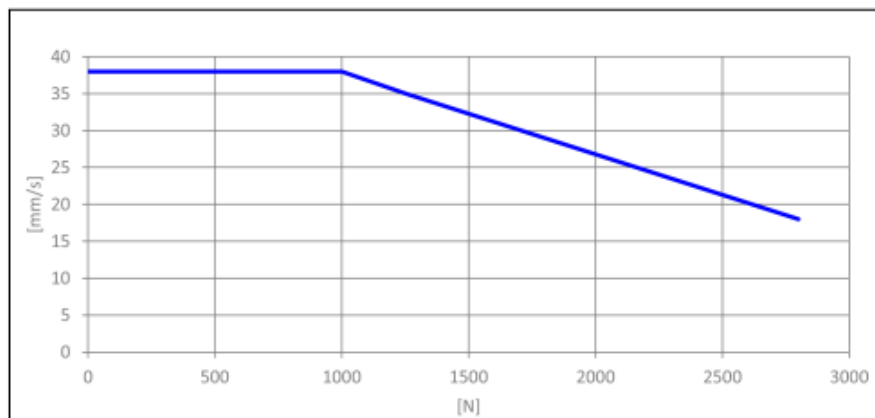


Figure 21: Maximum velocity for 4 DL11 connected

3.4.1 Lifting column for cobot

The market offers lifting columns with plates designed specifically for cobots from leading manufacturers such as Universal Robots. These columns offer an additional seventh degree of freedom, namely the vertical axis along which the column extends.

For example also LINAK offers a dedicated product shown in figure 22 Main benefits:

- Extended operating range of UR cobots to increase productivity and save costs
- No hardware/software upgrades required
- Direct positioning access within the UR control environment
- Vibration-free and virtually maintenance-free movement



Figure 22: ELEVATE lifting column for cobot from LINAK

This type of mechanism can be very convenient in cases like this where an elevation mecha-

Speed	up to 100 <i>mm/s</i>
Payload	up to 1000 <i>N</i>
Stroke	up to 1100 <i>mm</i>
Bending moment-static	3000 <i>Nm</i>
Bending moment-dynamic	1400 <i>Nm</i>
Weight	29 <i>kg</i>
Dimensions [LxWxH]	163 <i>mm</i> × 163 <i>mm</i> × 730 <i>mm</i>

Table 9: 'Elevate' main specifications

nism is necessary. There are models available for both the UR10e and UR20 cobots. Additionally, the advantage of using a single column connected to the manipulator is that it does not require lifting other battery-connected devices, thus eliminating the need for longer power cables that would enable translation, apart from the manipulator cable which is already several meters long by default.

However, the aspects that led to a different solution are mainly due to the composition of the mobile base. Firstly, the height of the column, even in the fully retracted position, does not allow it to be mounted on the mobile base because it would exceed the 2 *m* limit specified in Chapter 3.1.

Theoretically, partial insertion into the base is possible but not with this robot: the central part of the base is almost entirely occupied by the cylindrical frame and the rotational mechanism, and the column must be mounted directly beneath the cobot. Extending the outer frame to gain the necessary space is conceivable, but in this case, the robot would become too large. The rotation system must be centered, otherwise it would alter the robot's kinematic model. Therefore, extending the outer frame on one side would necessitate extensions on the other sides as well, and considering the bulk of the column, it is evident that the length and width limits would be exceeded.

If the concept of the internal frame housing the motor, battery and sprocket for rotation were to change and the column could be inserted at a maximum height from the ground of around 300 *mm*, then it could be a viable alternative to the system chosen to date.

Lastly, the column needs to be mounted on a stable surface, being possibly close to the edge of the robot could compromise the overall stability. But for this consideration, the static and dynamic behaviour of the specific model should be studied in more detail. Nonetheless, this remains a viable solution for a future robot designed for industrial environments, which allow greater navigation freedom due to generally larger spaces and access points.

Advantages	Disadvantages
Only one column Faster in lifting Less problems with wires Robust and designed for the cobot	Not enough space to mount it above or inside the base Wider frame needed Stability problem

Table 10: Pros and cons of lifting column for cobot

3.4.2 Controller

As a DL9 compatible controller, the company offers the **CBD6S**. It guarantees smooth operation and soft start/stop. The intelligent control box offers a compact and minimal-space design with



Figure 23: CBD6S Control box

a height of just 38 *mm* and a width that perfectly fits the motor-housing columns.

The CBD6S system can be built up as a single-column system; a parallel system with 2, 3 or 4 columns. Having 4 columns we need the 4-channel 300 *W* model.

The total dimensions are 265 × 38 *mm* as shown in figure 24, the weight is approx. 500 *g*.

CBD6S 300 W

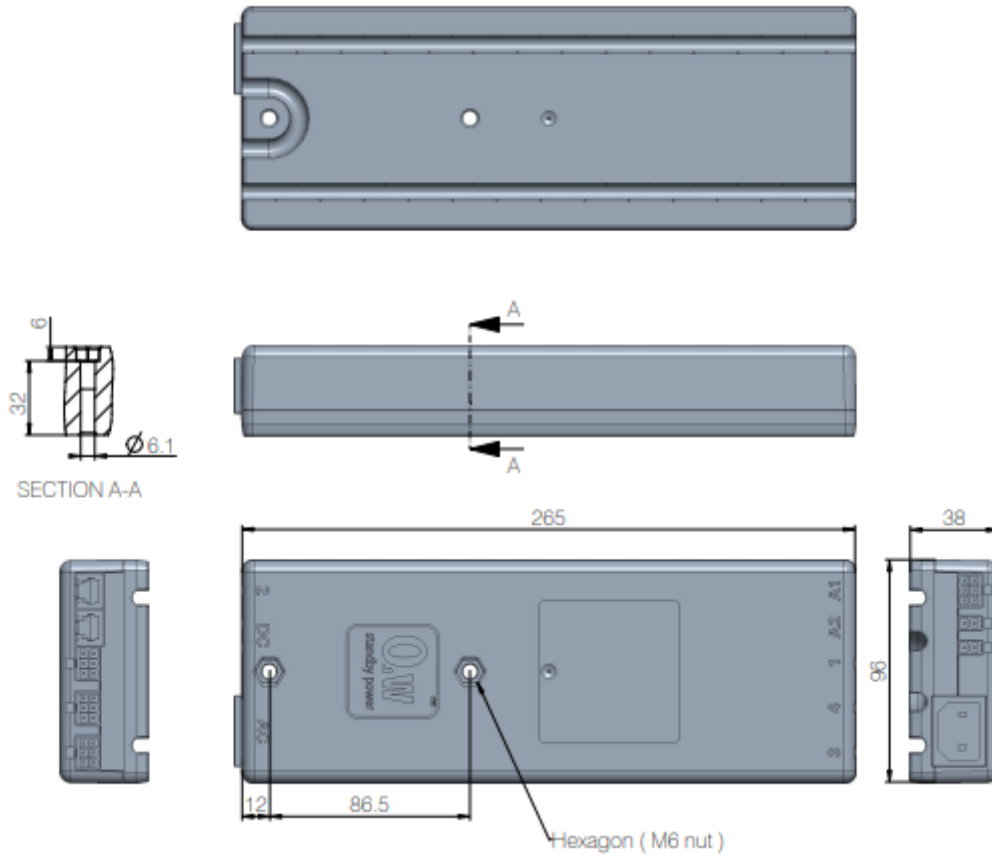


Figure 24: CBD6S draw

3.5 LiDAR

Light detection and ranging (LiDAR) technology allows for precise measurement of an object's distance and velocity. LiDAR works by emitting laser pulses towards a surface and measuring the time it takes for the reflected signal to return to the sensor. This time interval is used to calculate the distance between the sensor and the object. Knowing the speed of light, the system is able to determine distances with extreme precision, creating a detailed three-dimensional map of the area of interest.

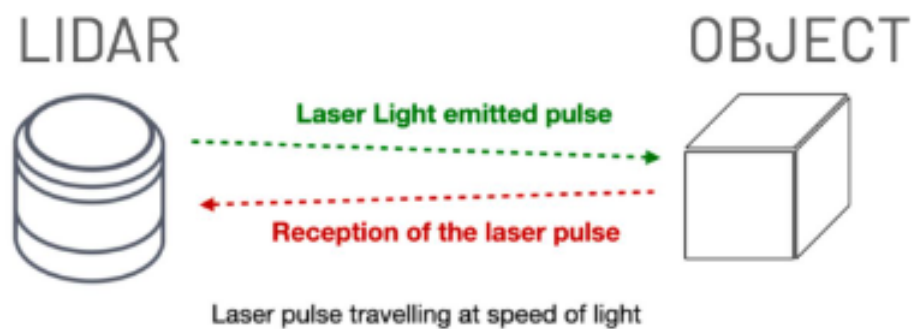


Figure 25: LiDAR functioning

The basic equation of its operation is:

$$d = \frac{c * \Delta t}{2} \quad (3)$$

in which d is the distance from the object, c is the speed of light and Δt represents the time light takes to reflect off a target that is illuminated by its light source.

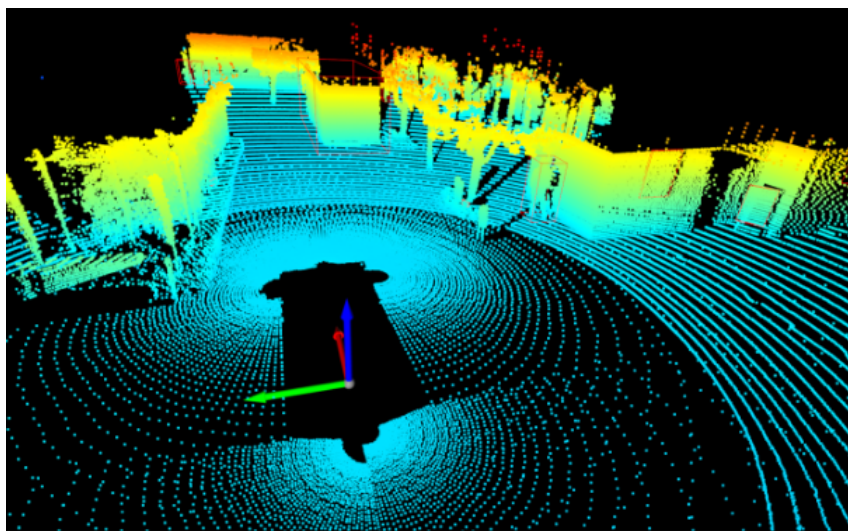


Figure 26: Example of 3D point cloud

The LiDAR system emits laser light toward a target and detects the reflected light to observe changes in wavelength and the arrival time of the reflected signal. By analyzing these measurements, it determines the distance, enabling the creation of a digital representation of the target. Given that light travels at an extremely high speed, LiDAR can quickly and accurately calculate the precise distance [21]. The combination of these measurements produces a 3D point cloud (fig. 26) representing the geometry of the detected surface.

Unlike the more established radio detection and ranging (RADAR) technology, LiDAR utilizes optical waves, which have shorter wavelengths than radio waves. This characteristic gives LiDAR the potential to achieve higher precision in 3D sensing [19]. Is a technology already used in many fields including robotics [25].

The main advantages are:

- High Resolution and Accuracy
- Speed of Data Acquisition
- Versatility

LiDARs are used are designed for outdoor use at medium to long distances or for obstacle detection in front of robots, so not many have a wide FOV (field of view) in both horizontal and especially vertical directions. For this project it is essential to have a wide vertical angle due to the need to map the entire building from floor to ceiling, presumably passing through narrow corridors.

For this technology, too, the choice was to rely on an industry leader such as *OUSTER* and precisely in the **OSDome** model in figure 27.

Table 11: LiDAR column specifications

Range at 10% (Lambertian reflectivity)	20 <i>m</i>
Range at 80% (Lambertian reflectivity)	45 <i>m</i>
Horizontal field of view	360°
Vertical field of view	180°
Vertical resolution	32, 64, 128 channels
Horizontal resolution	512, 1024, 2048 channels
Max points per second	5.2 <i>M</i>
Minimum range	0.0 <i>m</i> , at least 0.3 <i>m</i> recommended
Max frame rate	20 <i>Hz</i>
Min operating Temperature	-40°C
Max operating Temperature	60°C
Diameter	87 <i>mm</i>
Height with baseplate	107.77 <i>mm</i>



Figure 27: OUSTER OSDome LiDAR

The OSDome offers a complete 180° hemispherical field of view (the widest value among the major brands on the market), up to 20 m of range at 10% reflectivity, and high resolution. The OSDome delivers full coverage for indoor people tracking, and near-range detection for mobile robots and vehicles.

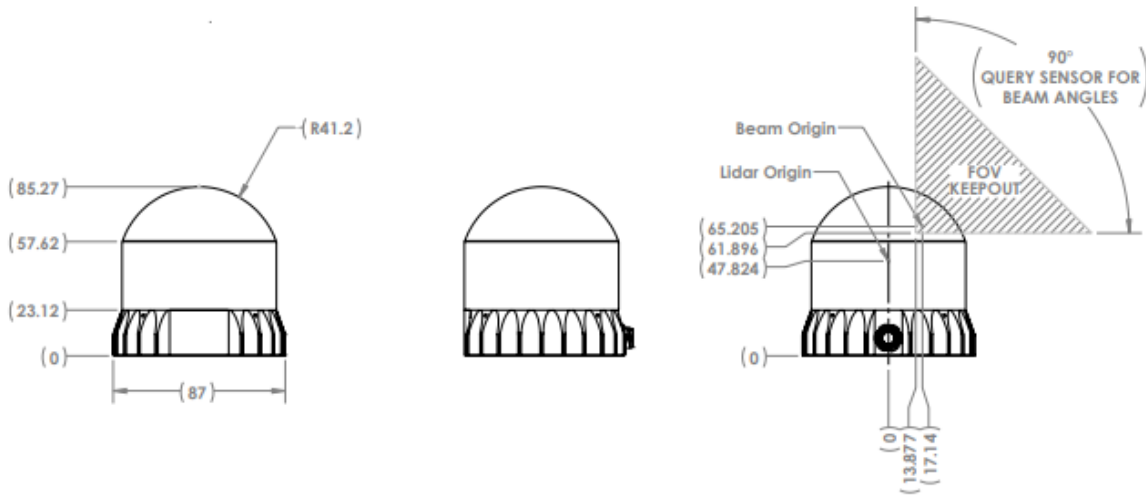


Figure 29: OSDome draw

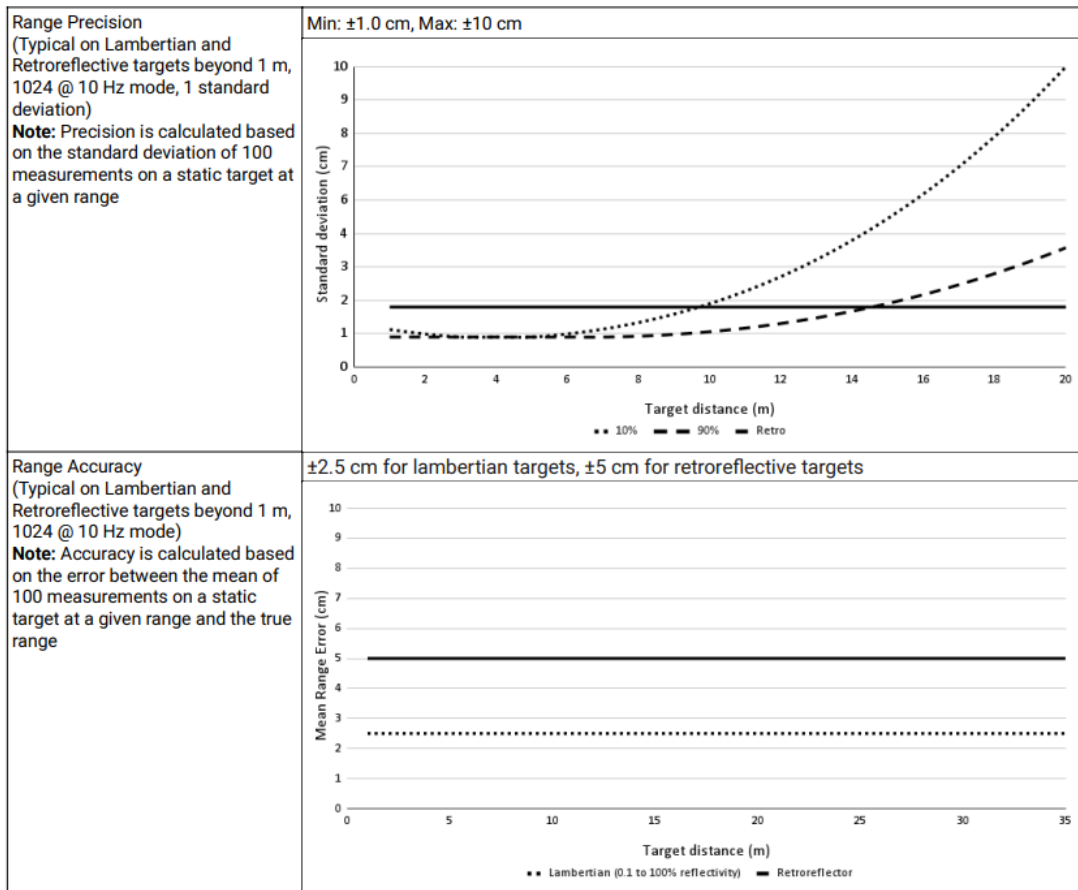


Figure 28: OSDome range precision and range accuracy

3.6 Camera

To be autonomous, the robot must be able to navigate and move in space. It can operate without human intervention, determining its route and safely avoiding obstacles. To function effectively, the robot needs a comprehensive real-time understanding of their surroundings, which is why the choice is to use depth cameras. Increasingly popular is the use of depth cameras for robots that navigate autonomously [7][20]. These devices are able to assess image depth through several methods [1]:

Structured light and coded light

Structured light and coded light depth cameras are similar but distinct technologies that project patterned light, typically infrared, onto a scene. The camera's sensor interprets the reflected light patterns to generate depth information. By comparing the expected pattern with the observed pattern, the system calculates the distance for each pixel. These cameras are most effective indoors and at short ranges, contingent on the emitted light's power. However, they can be susceptible to interference from other infrared-emitting devices in the environment.

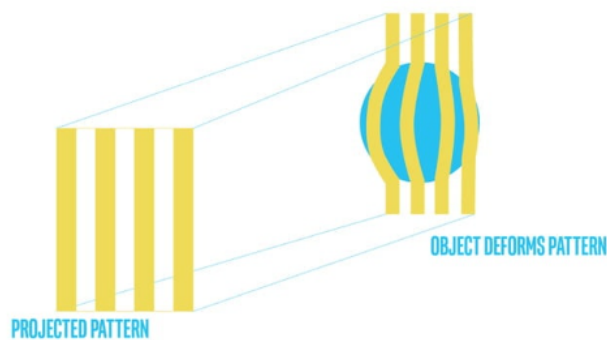


Figure 30: Working principle of structured and coded light camera

Stereo depth

Stereo cameras measure depth using any available light, including infrared. These cameras have two sensors spaced a small distance apart. By comparing the images captured by each sensor, depth information is obtained, similar to how human eyes perceive depth. The known distance between the sensors allows for calculating depth based on the disparity between the images. This technology works well in various lighting conditions, including outdoors, and adding an infrared projector enables depth perception in low light. Unlike coded light or time-of-flight cameras, stereo cameras can be used in any quantity without interference.

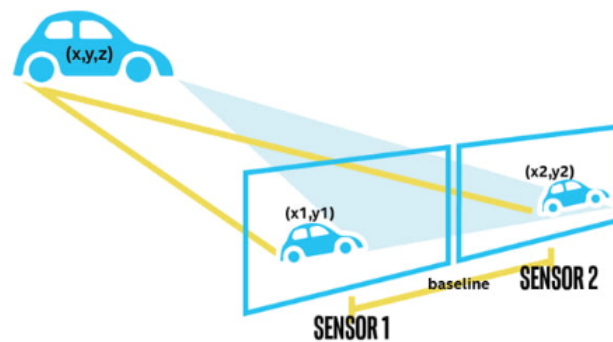


Figure 31: Working principle of stereo depth camera

Time of flight Lidar

In this case, they leverage the operation of LiDAR (see 3.5) by calculating the distance to targets based on the time taken for light to reflect and return to the sensor. However, they are susceptible to the presence of other cameras.

This precise depth information allows the robot to accurately understand spatial relationships and distances, enhancing its ability to move safely and efficiently through complex and changing environments. By quickly and accurately capturing depth data, these cameras enable the robot to make immediate, well-informed decisions, allowing it to adapt to environmental changes. This capability is especially important in settings where environmental factors can vary widely, such as different lighting conditions, surface textures, and the presence of moving obstacles.

Additionally, incorporating high precision depth cameras supports advanced functions like object recognition, scene understanding, and environmental interaction. Using LiDAR alone would fail to recognise the various types of surfaces or obstacles in the environment, which is why the use of this technology is essential.

Intel RealSense series cameras were chosen, in particular the model Dept Camera **D435i**. For versatile operation in different lighting conditions, the possibility of working with other devices without interference, reliability and compactness the choice is a stereo camera like this model.

Use environment	Indoor/Outdoor
Ideal range	3 m
Depth technology	Stereoscopic
Depth Field of View (FOV)	$87^\circ \times 58^\circ$
Minimum depth distance at max resolution	28cm
Length	90 mm
Depth	25 mm
Height	25 mm
Weight	75 g

Table 12: D435i specifications



Figure 32: RealSense Dept Camera D435i

As shown in the fig. 32 has very compact dimensions ($90 \times 25 \times 25 \text{ mm}$) and is also a model with IMU.

The inertial measurement unit (IMU) is employed to sense movements and rotations in six degrees of freedom (6DoF). An IMU integrates several sensors with gyroscopes to detect rotational and linear motion along three axes, including pitch, yaw, and roll. This technology is utilized in various applications such as gaming, pointing devices, and image stabilization. The combination of a wide field of view and global shutter sensor on the D435i make it the preferred solution for applications such as robotic navigation and object recognition.

3.7 Base

The mobile base is a fundamental constituent part of the robot. It is important to say that only the theoretical prototype of this component will be presented here, as a real project is still in the development phase. This is mainly composed of two main parts, an inner cylindrical part and an outer square-based frame as shown in figure 33.

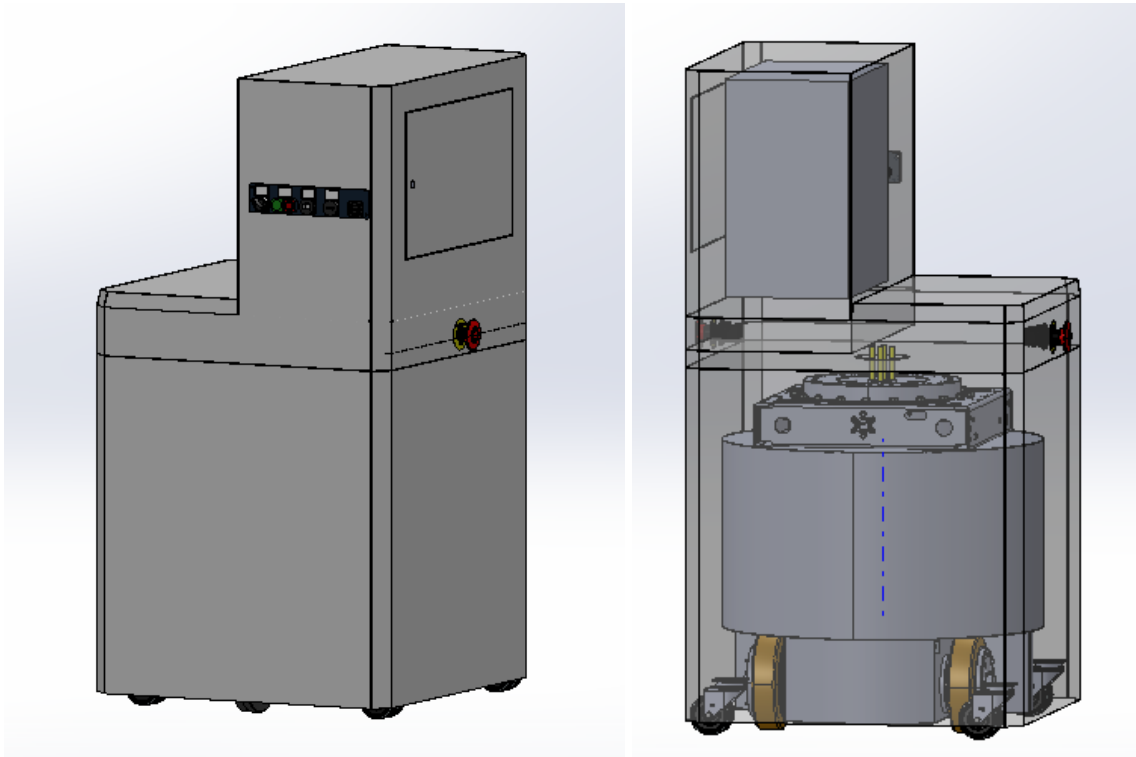


Figure 33: Mobile base first concept

In the upper section of the base, the manipulator will be positioned, while the adjacent compartment will house all the control units necessary for the manipulator, GPR, and LiDAR. Conversely, the cylindrical section will contain the motor that facilitates the movement of the base, the battery, and the remaining electronics.

These two sections are connected by a mechanism that permits the frame to rotate independently around its own axis. It is crucial that this component is centered relative to the base; otherwise, the entire kinematic system of the robot would be compromised (see chpt. ??).

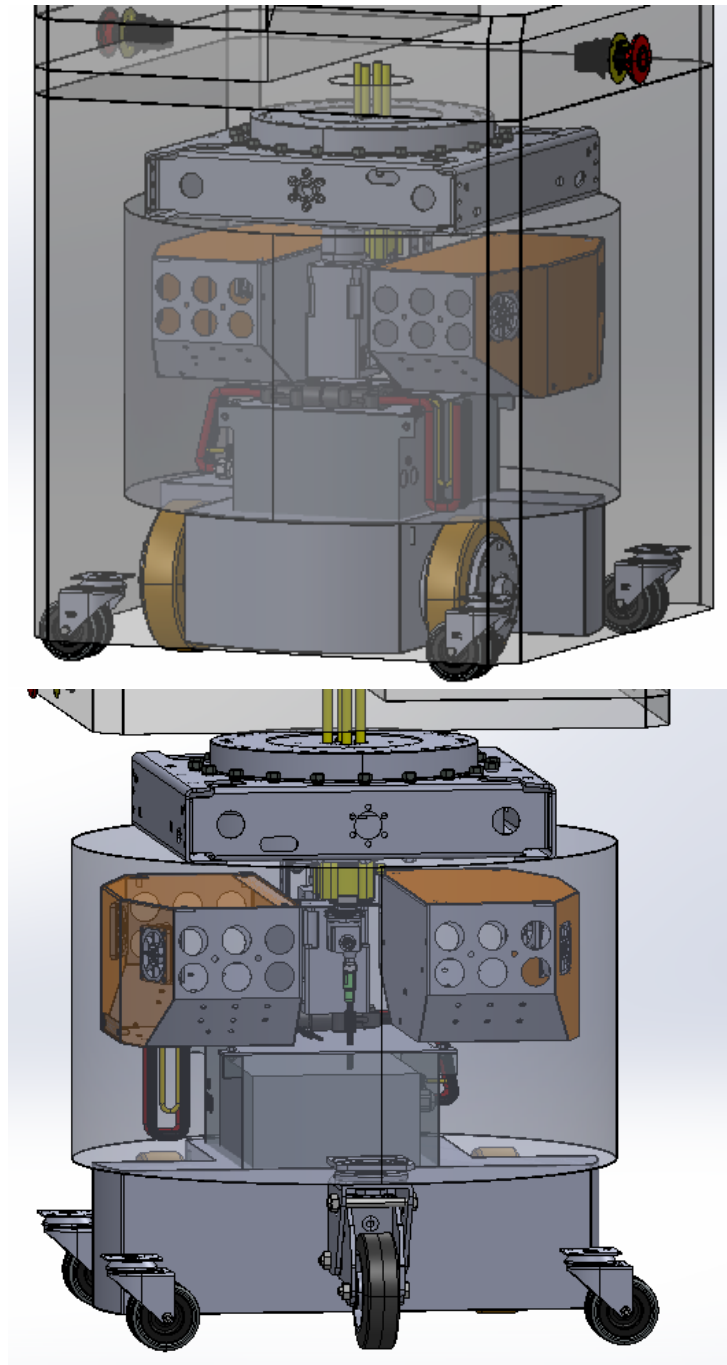


Figure 34: Cylindrical part of the mobile base with and without external frame

From bottom to top: the chassis with the two drive wheels and a castor wheel, the cylindrical structure containing the motor and battery, the rotation system connected to the outer frame

The kinematic structure consists of two driven wheels (in yellow in fig. 34) and one castor wheel as the primary base, with an additional four castor wheels supporting the external frame ,included to ensure stability and prevent tipping. To keep the outer part of the robot stationary

during movement, a motor with a slewing bearing is employed. The upper section houses the arm and control systems, which are connected to the electronic boxes in the base via a hollow shaft electrical collector. This configuration ensures that there is no cable rotation between the two sections.

Finally, a computer must be positioned in the cavity located between the upper part of the chassis and the mechanism that enables rotation. This arrangement facilitates the programming of the entire robot and ensures its autonomous operation.

3.8 Logistic issues and considerations

The description of the robot design in the following chapters takes into account the geometric constraints described in Chapter 3.1. However, it must be noted that logistical issues may arise when the robot is deployed in demolition sites.

Firstly, the robot is not designed to climb stairs. In residential buildings, such as large apartment complexes, this might be a minor issue since the floors often have a repetitive modular design, making it sufficient to operate on just the first floor.

Secondly, the robot does not consider passing over large obstacles. During the demolition of a building, it is common to encounter rubble or pieces of any material that makes up the walls, and the autonomous robot can detect and navigate around such obstacles in its path, but only where trajectory changes are feasible. Therefore, in narrow spaces, a preliminary cleaning action of the path should be considered, at least for larger obstacles.

Additionally, in sites designated for complete demolition, the power supply is usually cut off for safety reasons, meaning that elevators, if present, will not be operational. However, in partial demolitions, functional elevators may sometimes be available.

If it becomes necessary to explore floors other than the ground floor, alternative methods of transporting the robot must be employed, such as using lifting platforms or freight elevators from outside the building. The DISCOVER project aims to minimize human intervention, but it does not entirely exclude the possibility of creating an opening in the walls to allow the robot to enter from the outside, especially in buildings scheduled for complete demolition.

Another significant limitation of the project concerns industrial buildings. These structures can vary greatly in terms of layout and size, making it impractical to design a single robot model suitable for all scenarios. In office buildings and similar structures, floor dimensions are comparable to those of residential buildings. However, in industrial production environments, ceiling heights can easily reach between 4 and 5 meters or more, as seen in warehouses. Considering that, where feasible, ceilings can be inspected using the GPR probe from the floor above or from the roof (if accessible), it is evident that the robot described here will have limitations in reaching higher walls. Nonetheless, given the larger maneuvering spaces in these buildings, it is possible to design a larger robot with a wider base and a longer robotic arm to operate in more expansive areas, possibly accompanied by more robust and longer lifting columns.

Last but not least, doors represent an additional complexity for the robot's autonomy. Even if all doors are open, the robot must be capable of moving them to completely scan the wall areas covered by these doors. Currently, the robot is designed with a single robotic arm equipped with

the GPR antenna, which is not suitable for pushing a door. If the robot encounters a completely closed door, an end effector capable of opening it using handles or knobs would be necessary. This poses a significant challenge to the robot's autonomy. Therefore, it is important to note that the project assumes all doors in the buildings have been removed.

Moreover, the DISCOVER project aims to recover materials from demolished buildings, making it feasible and reasonable to consider salvaging old doors as well. If it is not possible to prepare the work site in advance by removing the doors, an additional robotic arm could be considered, capable of grasping objects and thus opening and closing all major types of doors.

4 Base kinematics and static stability

This chapter will address the kinematic behavior of the mobile base and the overall stability of the robot in static conditions. It is not the aim of this document to provide a detailed discussion of the physical and mathematical models. Instead, the subsequent sections will offer a conceptual description or specific (limit) cases. Upon completion of the project for the mobile base with all mechanical and electrical components, a more in-depth study of the robot's mechanical behavior can be conducted if deemed necessary.

4.1 Statics

Regarding statics, as there is not yet a definitive project for the mobile base and other structural components such as plates and supports, this document will not analyze the stress and moment distribution in the material. Instead, with the assistance of *SOLIDWORKS* software, only the center of mass (COM) of the entire robot in various configurations will be analyzed to ensure it remains within the perimeter of the base. As shown in the figure, if the center of mass remains within these limits, it can be stated that the robot in a static position is stable.

The weight of the non-commercial components has been estimated. The cylindrical mobile base, which includes the motor, battery, rotation system, and electronic components, has been estimated at 150 kg. The external frame, both the lower and upper parts, is assumed to be made of aluminum, and its weight has been realistically estimated based on its density.

The weight of the various components is therefore reported in [13](#).

As can be seen in the figures [35](#) and [36](#), the weight of the mobile base, outer frame and columns is much more decisive than the weight of the cobot for the total centre of mass of the robot. The COM is clearly within the perimeter of the outer frame, which will be supported by 4 wheels at the vertices, so no problems of static stability are expected.

In any case, should a stability issue arise, it is possible to place a counterweight inside the base to balance any potential weight imbalances.

Component	Weight
Mobile base*	150 <i>kg</i>
External frame (lower)*	25 <i>kg</i>
External frame (upper)*	20 <i>kg</i>
Cobot	33.5 <i>kg</i>
Column	7.5 <i>kg</i> each
OEM control box	4.5 <i>kg</i>
Computer*	4 <i>kg</i>
Gpr	0.5 <i>kg</i>
Column control box	0.5 <i>kg</i>
Total	264 <i>kg</i>

Table 13: Component weights

* Estimation, the component is not yet designed

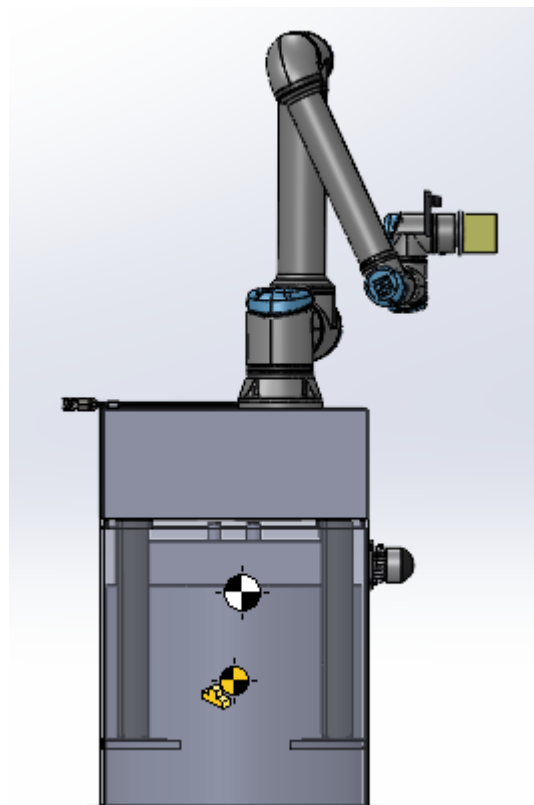


Figure 35: Center of mass in rest configuration
 In yellow the mobile base COM, in white the total robot COM

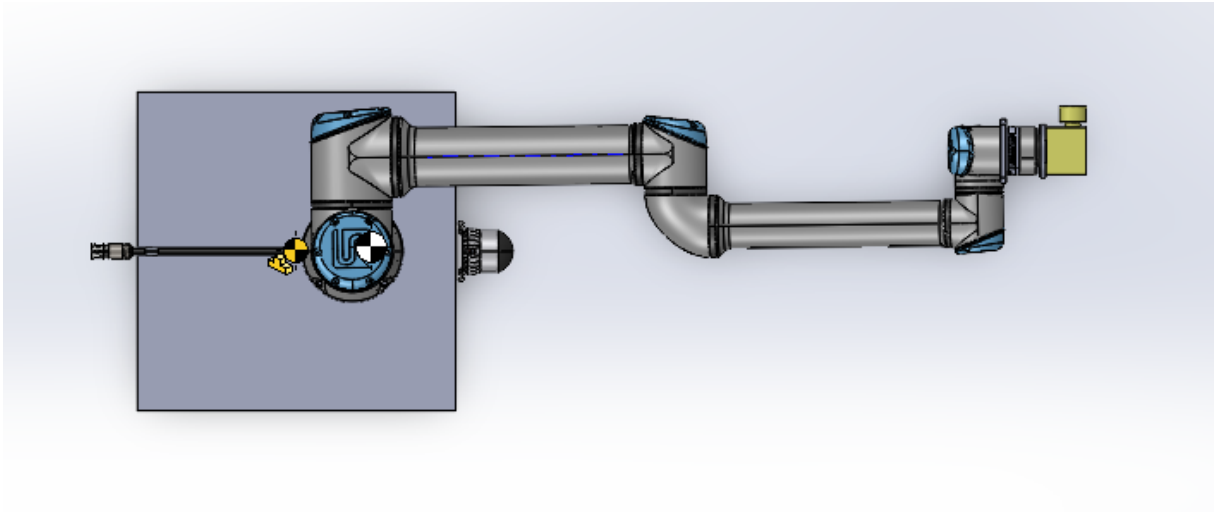


Figure 36: COM in maximum horizontal extension
In yellow the mobile base COM, in white the total robot COM

4.2 Base kinematics

A wheeled mobile robot (WMR) has three coordinates in the plane (x, y, θ) . An omni-directional WMR can be defined as a robot that allows any trajectory in the plane starting from any configuration (x, y, θ) (fig. 37).

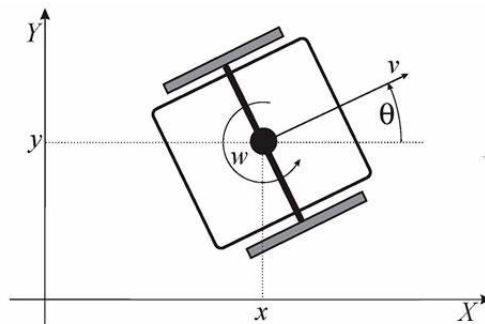


Figure 37: Wheeled mobile robot scheme in bidimensional space

This robot handling system follows that of a MOBY platform project that was developed and patented at the Polytechnic University of Catalonia (UPC) [9]. It is an offset-differential robot that allows omnidirectionality using standard wheels, which allow stability and higher loads than the latest omni-wheels (fig. 38) used for some mobile robots [23]. MOBY's model description and its kinematic and dynamic behaviour are well explained by Badia Torres, Perez Gracia and Domenech-Mestres in [4].

In this document, the mathematical model of the system will not be addressed in detail; instead, the focus will be on highlighting the key aspects and advantages that justify its use for this new



Figure 38: Example of omni wheels

robot.

In contrast to a differential wheeled robot, where the two driven wheels can rotate independently in both directions and the machine's steering is controlled by the difference in wheel speeds, this system features an additional actuated rotation around an axis that is perpendicular to the plane of motion and offset from the wheels. Essentially, it combines an offset differential robot with a vertical rotation around a centered axis. For the differential robot, the instantaneous center of rotation is always located on the line connecting the axes of the wheels, as illustrated in the figure. The system's third vertical axis allows this line to be oriented arbitrarily while maintaining an independent orientation of the robot's body. Additionally, a caster wheel is mounted to the robot's base for added stability. [4]

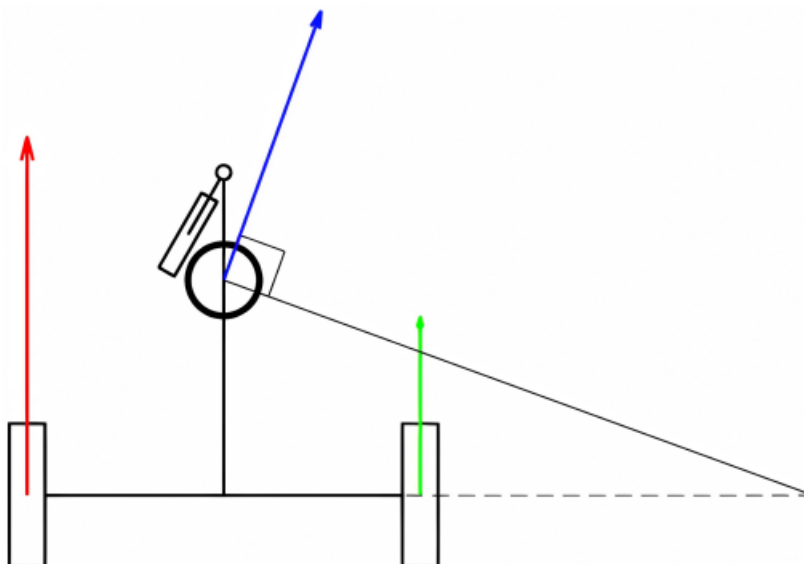


Figure 39: Kinematic model of the robot

The figure 39 shows the instant velocity of the center of the robot (in blue) is a function of the

velocities of the wheels (in red and green).

The external frame can therefore rotate independently of the wheel axis and is equipped with four smaller wheels solely for the stability of the entire robot, being irrelevant for the overall kinematics.

The principal advantage of this system is its ability to translate the robot's instant center of rotation arbitrarily along the line of the axis of the two wheels. This feature provides maximum freedom of movement, enabling the robot to follow any trajectory within its operational space. Furthermore, this configuration permits the use of traditional wheels, which allow stability and higher loads than the latest omni-wheels (fig. 38) used for some mobile robots [23].

There are, of course, issues with this system, particularly in terms of driving stability, as demonstrated by Yun & Yamamoto [26] when the two wheels are positioned at the front and thus "pull" the chassis instead of "pushing" it. However, these concerns are addressed in [4], where the problem is detailed and methods for mitigating it are explained.

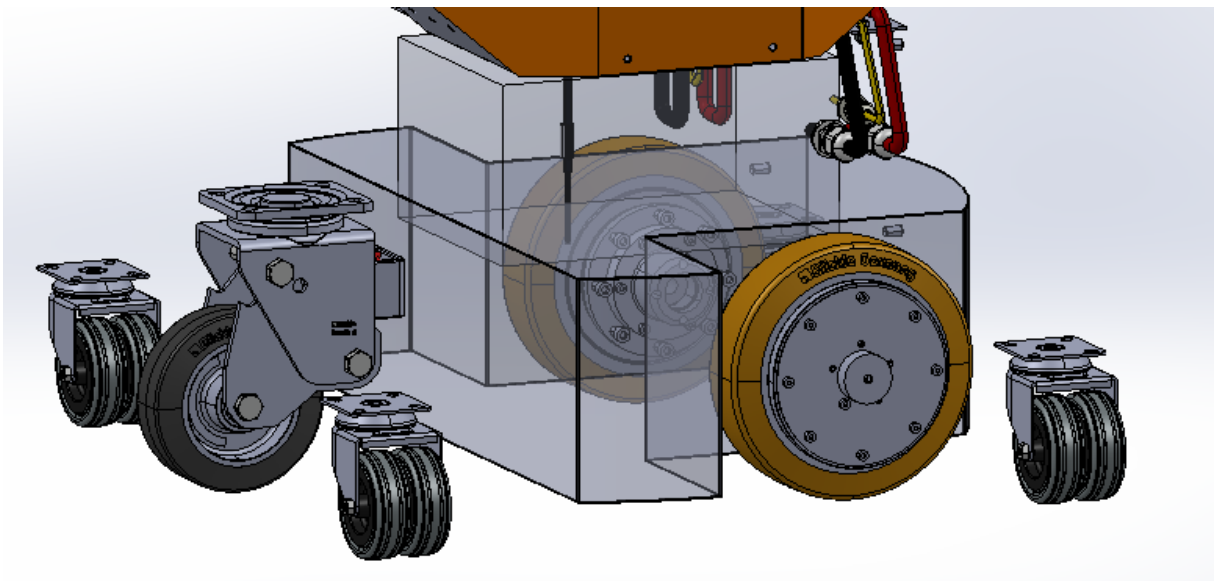


Figure 40: Chassis scheme

In yellow the two driving wheels and in the front the castor wheel; the 4 other castor wheels support the external frame not represented here. A small shaft indicating the axis of rotation is also visible in the figure

5 Final design

In this chapter, the final design concept is presented, considering that the entire base is still in the design phase. The following figures take into account estimated and currently deemed realistic limit dimensions. Any substantial differences in these dimensions may lead to significant modifications in the design. The main discriminating factor is the internal cylindrical base, which contains the essential components for the robot's mobility and energy autonomy.

Being nothing more than a guideline for a provisional design, which requires further information to be defined more specifically, technical drawings will not be provided as they would have no actual significance. Instead, limit or realistic dimensions will be provided to be followed in the next phases of the actual design process. Additionally, the choices for each component and its placement within the robot will be justified.

An important aspect to specify is that the proposed design does not include drive or caster wheels, as their specifications will need to be calculated based on the final project (weight and dynamic model of the robot). Nonetheless, the frames, both the external and internal ones, represent the total height of the robot and should therefore be considered inclusive of the wheels.

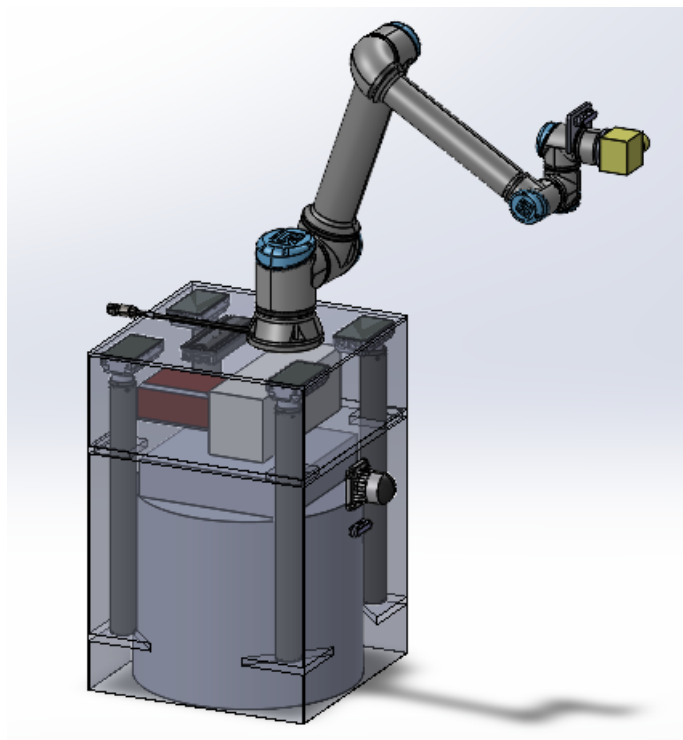


Figure 41: Full robot concept

5.1 Cilindric frame

The cylindrical component (fig.42) represents the mobile part of the robot, which will house the motor, battery, and any electronic parts. Additionally, it includes the chassis 3.7 with two drive wheels and a caster wheel, which determine the robot's kinematic behavior 4.2. The four bars extending from the top illustrate the connection to the external frame that facilitates its rotation. The dimensions provided are considered realistic estimates based on design experience with similar components.

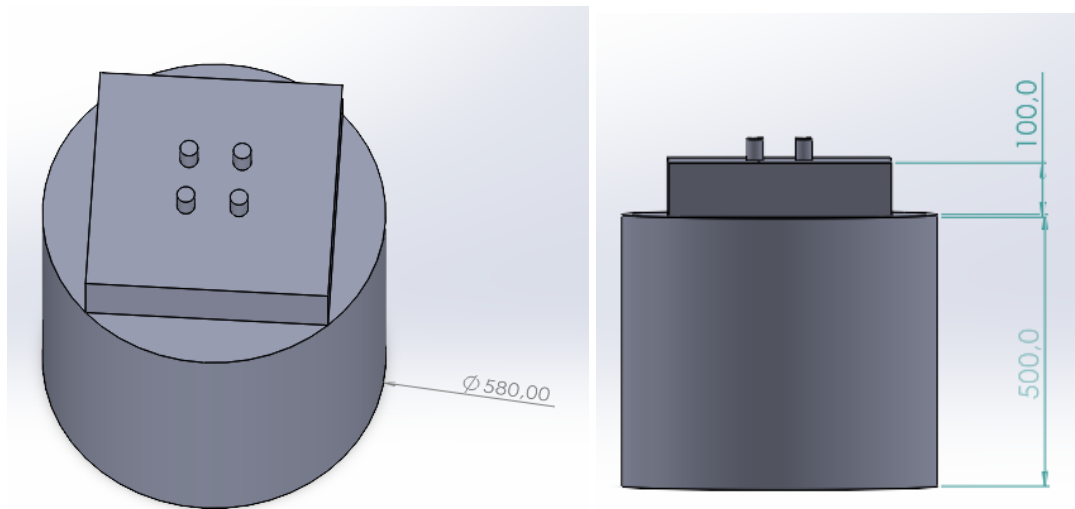


Figure 42: Cilindric frame dimensions

5.2 External frame

the External frame is made up of two parts: a lower one (fig. 43 containing the mobile part of the robot (cylindrical frame) and an upper one containing the manipulator and raised together with it. From the lower frame, placed on special supports, start the 4 columns that allow the vertical movement of the robot. Between the two frames are the manipulator control panel, the column control panel and the computer that manages the entire robot.

The two frames have the same dimensions in width and length. In the proposed concept they have a square base. This maintains greater symmetry in the robot and improves manoeuvrability. Having such a base one could consider the robot without a preferred direction, in reality this is not the case for two reasons: the Lidar placed at the front of the robot and the manipulator not positioned in the centre of the base. The reasons are explained in chapters 5.4 5.5. The maximum width of 600 mm is due to the minimum opening of interior doors as discussed in chapter 3.1. The lower part will then be provided with supports on which to mount the columns (fig. 45) and holes at the top to allow them to pass through.

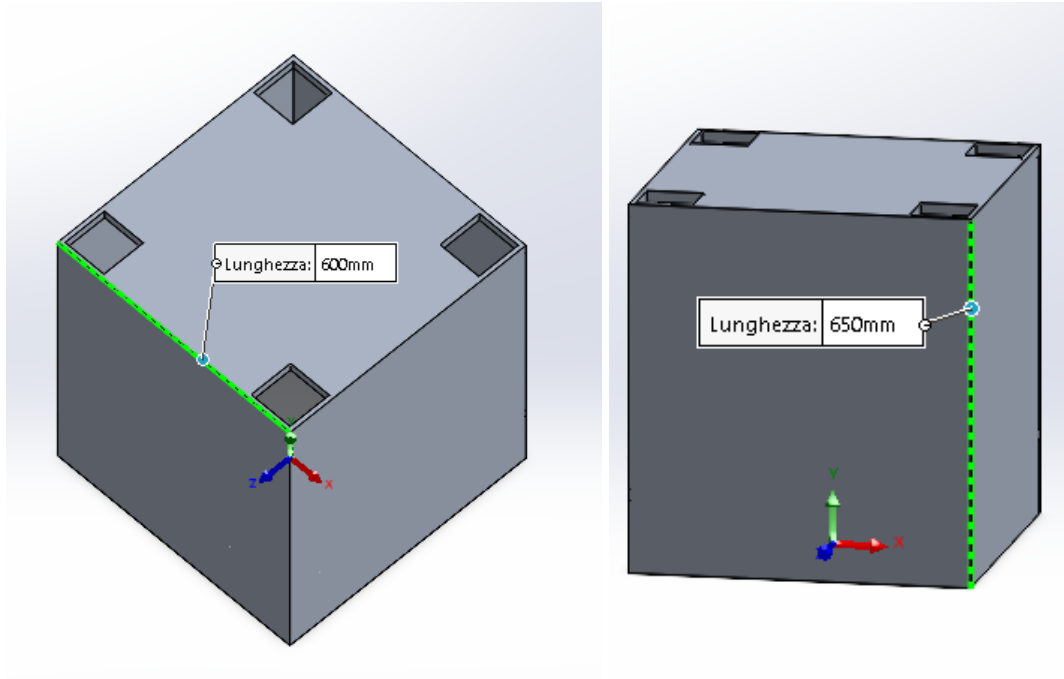


Figure 43: Lower frame dimensions

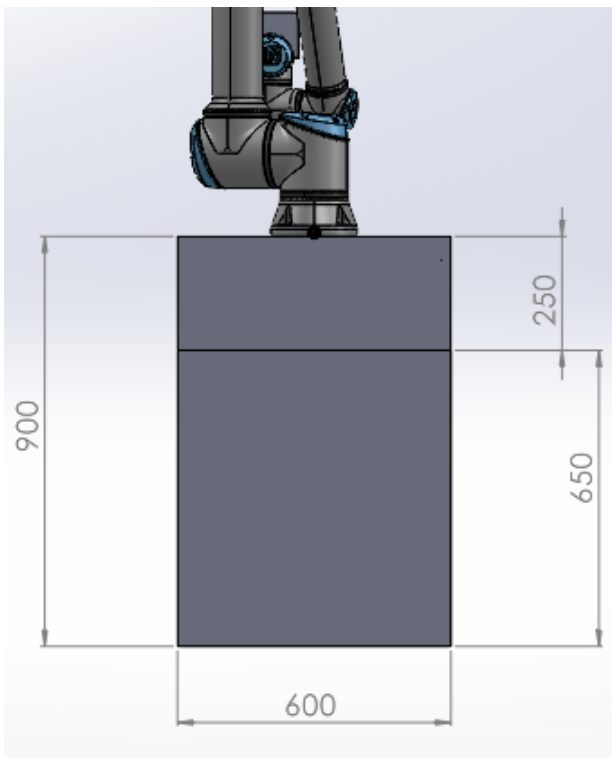


Figure 44: External frame dimensions

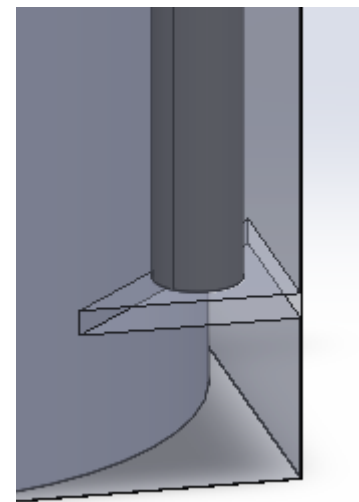


Figure 45: Example of base support

5.3 Controller boxes

Between the two parts of the external frame, the control box for the manipulator, the control box for the columns, and the computer that will be programmed to make the robot operational are positioned.

For the computer, a model used in a similar robot within the department was taken as an example (fig. 47) and in the model was considered to be $200 \times 150 \times 100 \text{ mm}$ in size.

As the figure 46 show, with these frame dimensions, it is possible to fit all the components in the available space without any interferences, also considering the columns and motor housings.

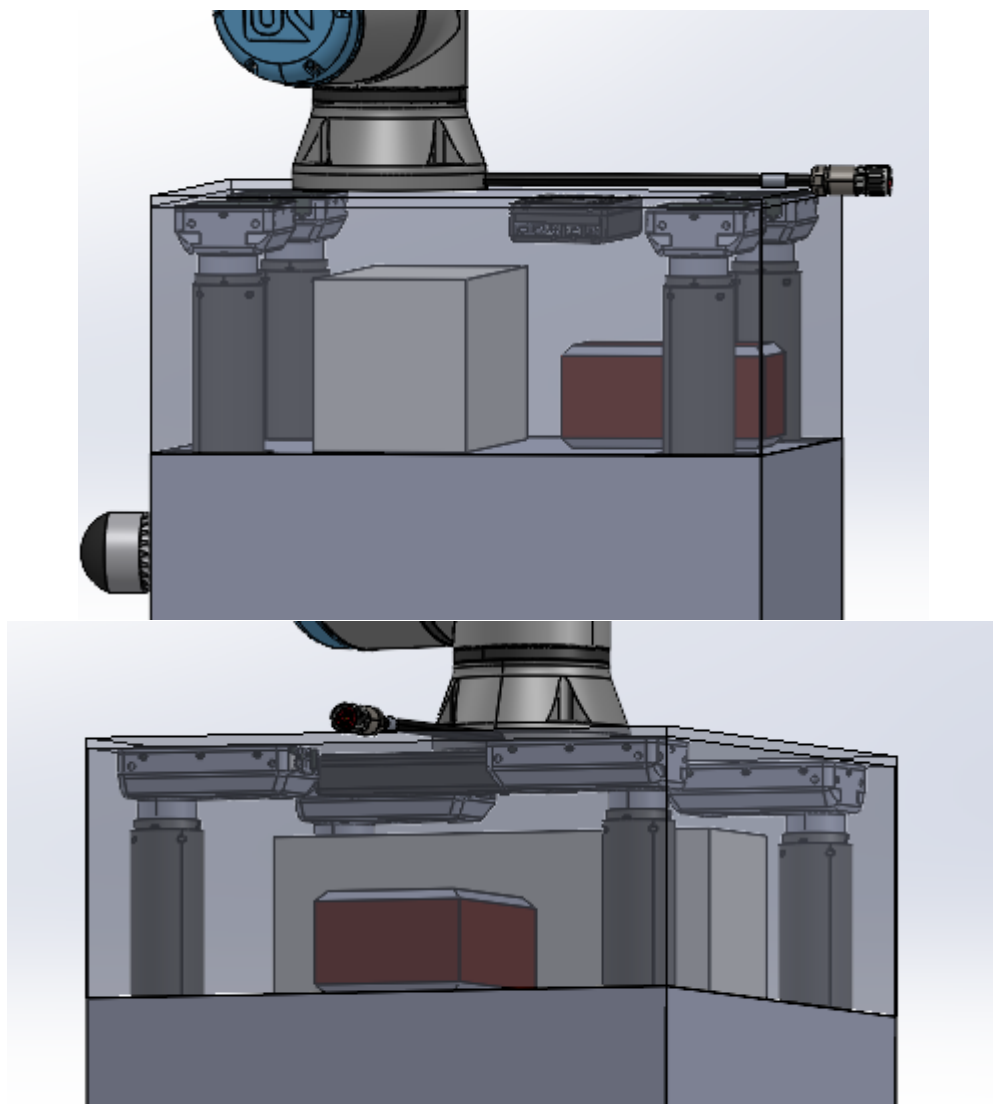


Figure 46: Possible configuration of controllers

In white the manipulator control box, in red the pc, in black mounted on the upper frame the columns controller



Figure 47: Example of pc box

Considering the two greatest heights (168 mm for OEM control box and 46 mm for column motor housing) the minimum upper frame height that allows all the component to be inside is 214 mm . In case it is not possible to leave space between the two parts of the frame, the cobot controller can be mounted on the top of the robot. In this configuration, the upper frame of the base, which is currently designed as a square plate, will need to be modified with a hole to ensure that the control box is not lifted together with the cobot.

5.4 LiDAR

The robot, intended to navigate through rooms and narrow spaces, may encounter difficulties in scanning every point on the wall. To address this issue, we have sought a LiDAR with a larger Field of View (FOV). OS Dome, with its hemispherical FOV (fig. 48), enables a comprehensive view of the space in front of the robot. Therefore, the design plans to mount the device at the front of the base. Ideally, for safety and protection of the expensive LiDAR, it would be preferable to position it within the perimeter of the base. However, this particular placement ensures complete mapping capability throughout the robot's path.

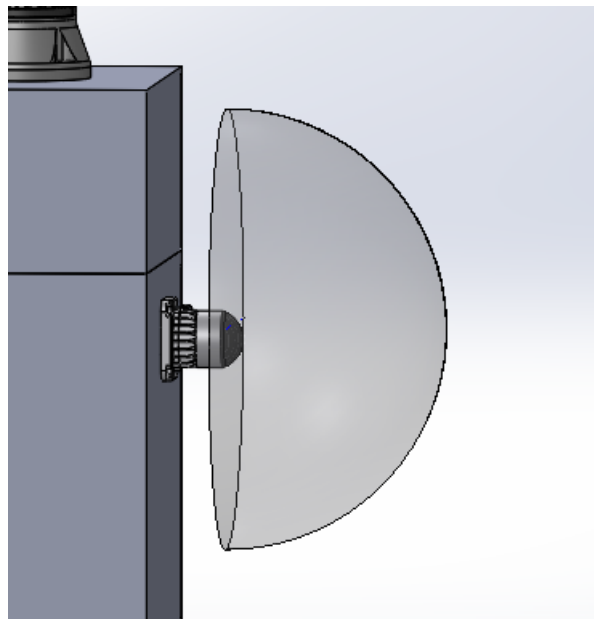


Figure 48: Representation of LiDAR FOV

Given that impacts of the robot with walls or obstacles are not expected but cannot be entirely ruled out, it is essential to consider protective measures for the LiDAR. Two alternatives have been proposed for safeguarding the LiDAR.

The first involves mounting a transparent shield over the device. Tests conducted by the company have shown no significant interference or data loss when using the LiDAR behind glass.

The second idea is to use a protective frame that does not completely cover the device. This approach will require programming the LiDAR to ignore data related to the frame's presence.

Both options are feasible, but the most effective solution can be determined through testing once the LiDAR becomes available.

5.5 Cobot

The position of the cobot on the base is crucial in determining its mobility and reach. As discussed in Section 4.1, its weight poses no static stability issues, hence there are no strict distance constraints from the edge of the base to adhere to. In this design, it has been mounted 100 mm from the front edge of the frame (fig 50). This primarily affects the maximum height of the entire base. The robot exhibits high agility with 360° mobility at each joint, yet the presence of the base restricts downward movement. The issue arises from contact between Link 1, between the shoulder and elbow joints, and the frame.

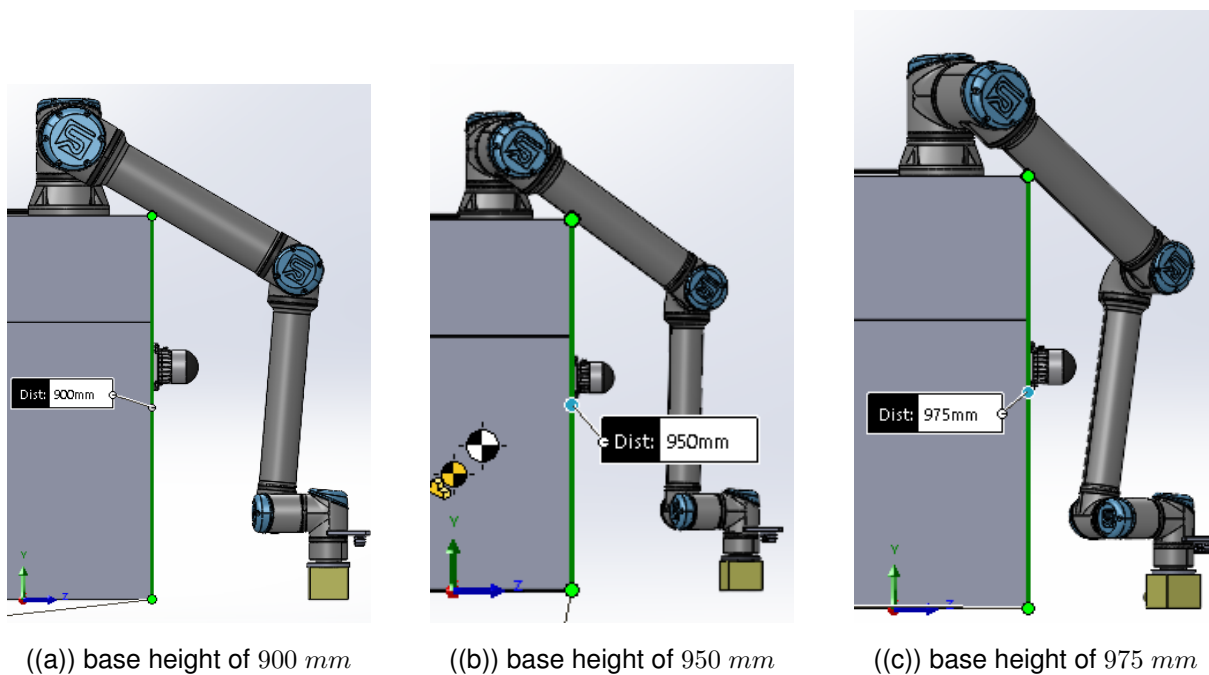


Figure 49: Cobot scanning the ground

As can be seen in the figure 49, by increasing the total height of the base, the cobot continues to reach the ground but loses mobility; in fact, notice how the base is forced to rotate as it increases to allow movement. This leads to limited operability. For this reason it is recommended not to exceed a total height of 950 mm, always considering this specific position of the cobot on the base.

Some useful lengths are given such as the height of the robot with the manipulator in the rest position (link 1 vertical) of approx. 1750 mm (fig. 51) and the maximum distance that can be reached while scanning the floor of approx. 580 mm (fig. 52).

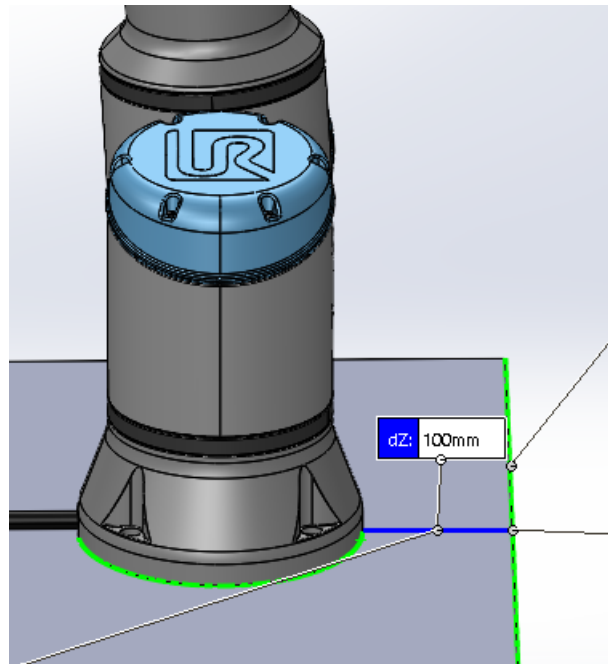


Figure 50: Cobot distance from the edge of the base

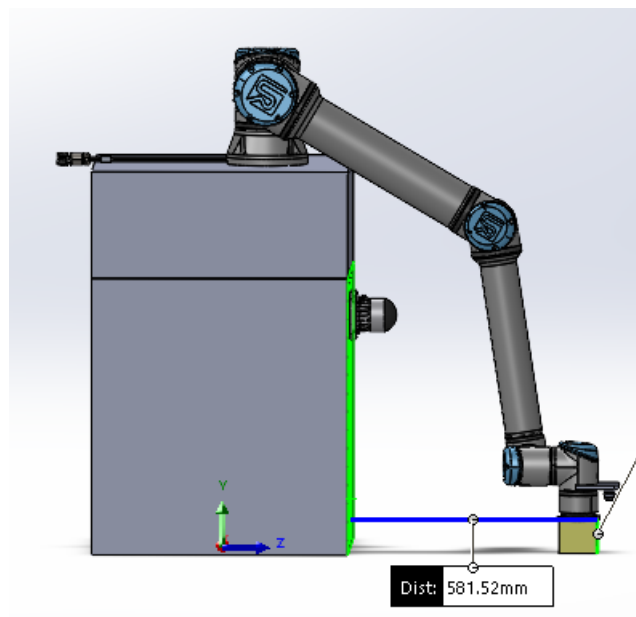


Figure 52: Maximum extension touching the floor

The maximum height that can be reached without a lifting movement (at a distance of 150 mm from the front of the base in order not to hit the LIDAR) is approx. 2400 mm (53).

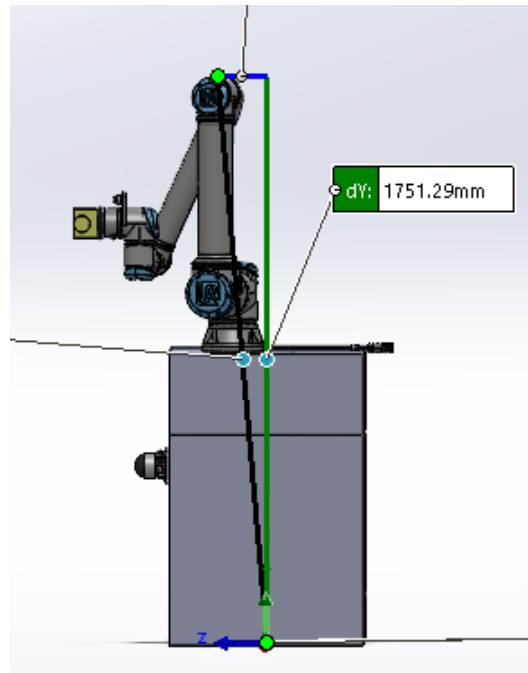


Figure 51: Robot height in rest position

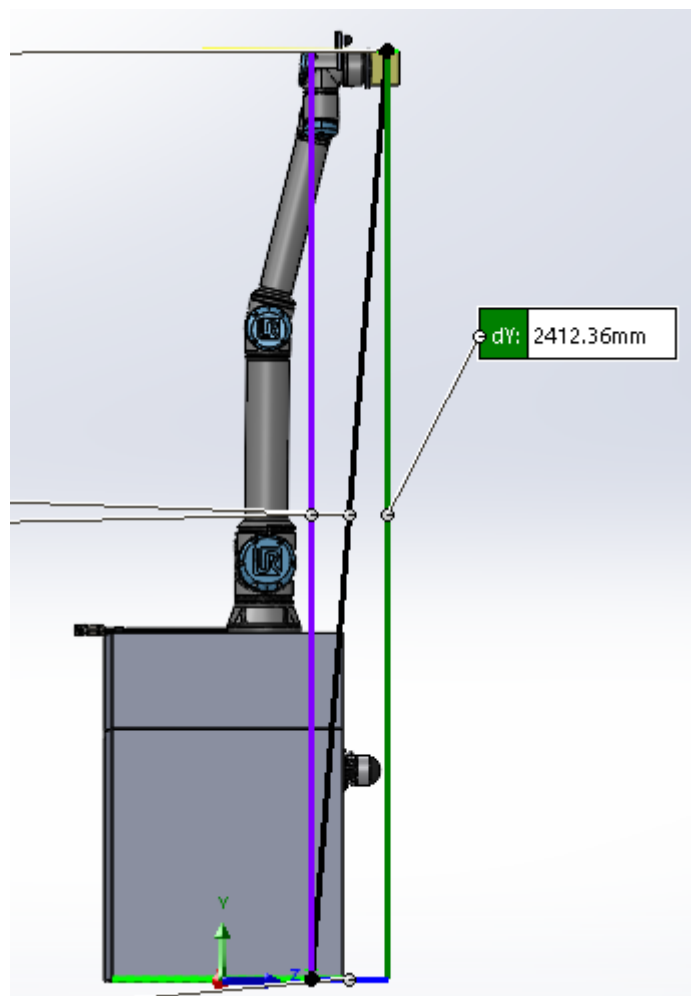


Figure 53: Max height without a lifting

5.6 Lifting column

Four columns are used for the vertical movement of the plate. They are fixed on lower frame supports (fig. 45) and connected under the upper frame plate.

The columns have a stroke of 965 mm , which brings the maximum height of the base to approximately 1865 mm . Consequently, the manipulator can reach approximately 3350 mm (54).

The threshold of 3 m is abundantly exceeded. these remain theoretically attainable measurements, but it is not recommended to extend the columns as far as possible because the system may present unexpected instabilities. With these extension possibilities, there should be no problems, especially in civil buildings.

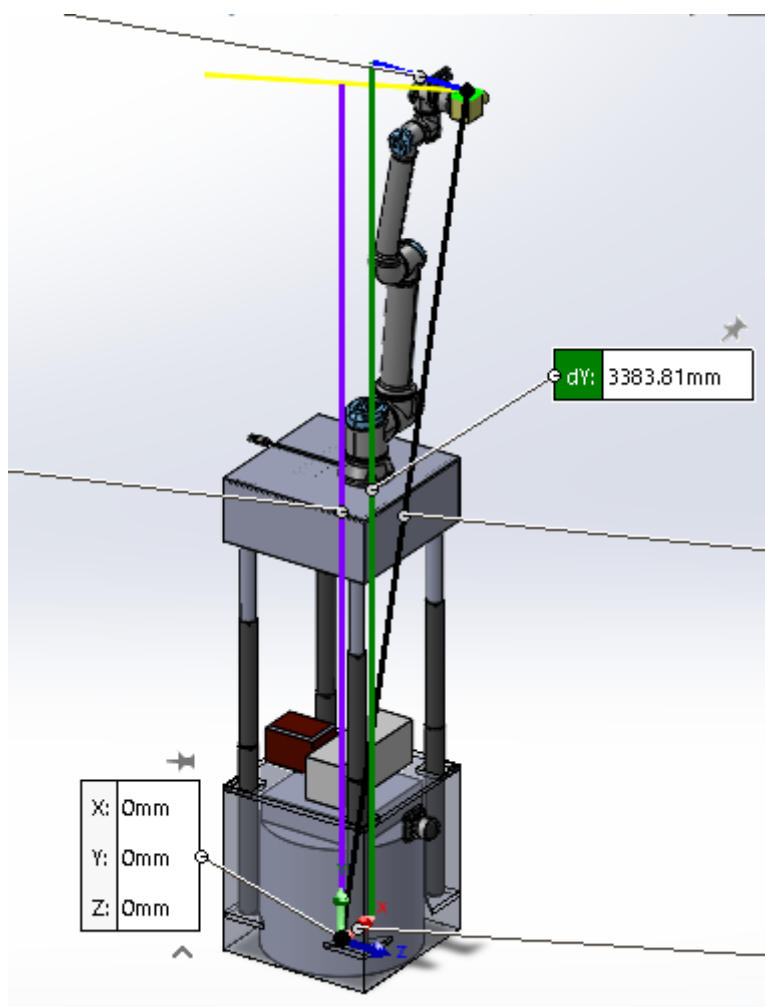


Figure 54: Maximum reachable height

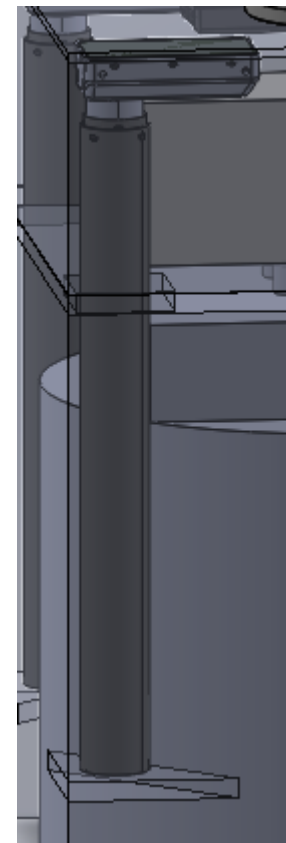


Figure 55: Lifting column in the base

As seen in Chapter 3.4, each column can support 600 N and 100 Nm of bending moment, so having 4 columns the total loads are 2400 N for axial load and 400 Nm for bending moment.

Considering the weight of the cobot (35 kg, including Gpr and camera) and the estimated weight of the upper frame (20 kg), we have a total of 55 kg, which translates to:

$$55 \text{ kg} * 9.81 \frac{\text{m}}{\text{s}^2} = 539.6 \text{ N} \quad (4)$$

From the equation, it is immediately evident that the weight of the upper part of the robot is not a problem at all.

As for the bending moment, only the cobot is considered, as it is the most problematic component due to its ability to shift its center of mass away from the base. Considering its worst configuration, where it is fully extended in a horizontal position, the applied bending moment is calculated as follows:

$$35 \text{ kg} * 9.81 \frac{\text{m}}{\text{s}^2} * 0.65 \text{ m} = 223.2 \text{ Nm} \quad (5)$$

In the equation, the center of mass is considered to be at the midpoint of the robot's maximum extension (1.3 m). In reality, the center of mass is closer to the base than to the last joint as shown in fig. 56, but considering the GPR antenna and the camera with the support, a more conservative calculation is preferred.

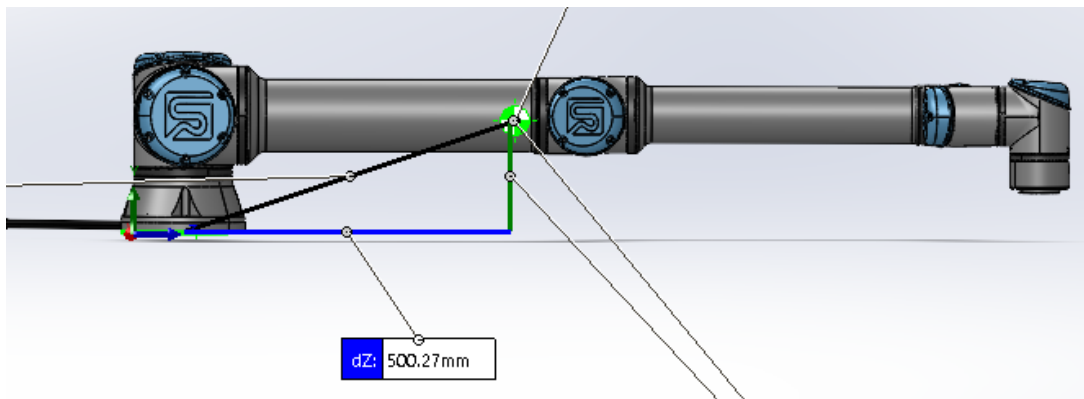


Figure 56: Cobot center of mass

What results is that more than 2 columns are needed to support the cobot. Additionally, having one column at each vertex ensures greater stability during movement and better distribution of the loads.

5.7 Gpr and cameras

The gpr antenna is connected through a special holder to the last link of the cobot as an end effector and the camera is mounted just before it through a plate. The camera must be able to see beyond the gpr in order to understand and identify the elements of the surrounding environment. Thus the manipulator can be programmed to move as required.

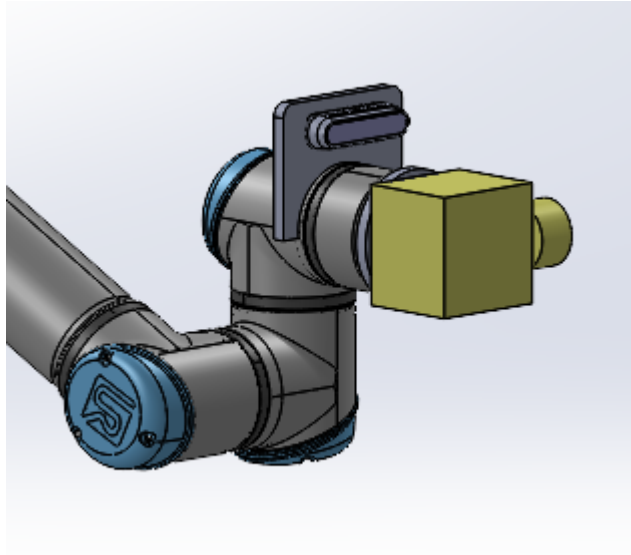


Figure 57: Camera and GPR mounted on the cobot

In figure 57 gpr is shown in yellow in its stated dimensions, the cylindrical part represents the wheel that enables its operation.

The chamber must be calibrated according to the distance at which it will be mounted.

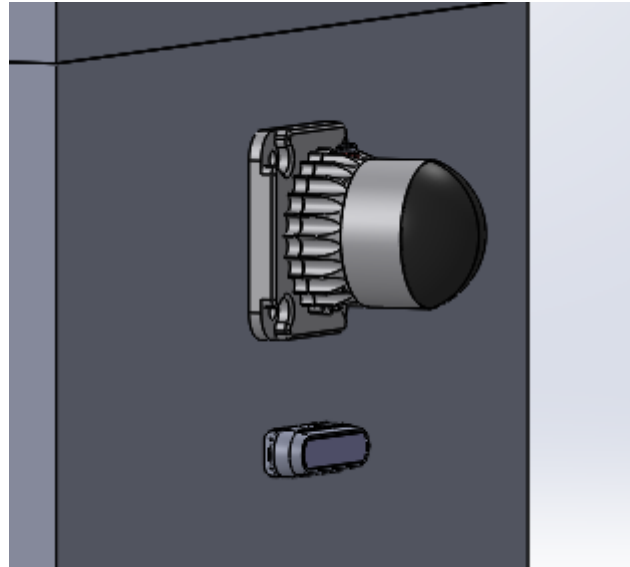


Figure 58: Camera on the front of the base

A second camera is provided on the front of the robot to enable identification of surrounding obstacles and thus the robot's smooth autonomous driving [58](#).

In the figure, the camera is placed below the Lidar for demonstration purposes only. Despite not falling within the latter's field of view, it can be mounted inside the base, with holes made specifically for the lenses. Thanks to its operating principle, it is not affected by the presence of other devices emitting light signals (chpt. [3.6](#)).

These types of cameras are not expensive, especially compared to other components of the robot such as the cobot or the Lidar. Therefore, in addition to these two cameras necessary for the movement of the base and the cobot, it is advisable to use additional cameras on the other sides of the base (or at least on the back). This decision will depend not only on the project budget but also on the level of safety required, as people may be present near the robot during its navigation. Thus, a broader view of the surrounding operational area is necessary to avoid unwanted accidents.

6 Conclusions

This thesis has explored the potential of robotic technology to transform traditional demolition practices through the development of a mobile robot integrated with Ground Penetrating Radar (GPR). The robot can perform autonomous scans autonomously providing essential data for Building Information Modeling (BIM) thanks to a LiDAR and supporting the demolition process. The successful deployment of this technology not only promises to improve operational efficiencies but also significantly enhances worker safety by reducing human exposure to potentially hazardous demolition environments. The implications of this research extend beyond technological innovation, offering a path toward more sustainable demolition practices by facilitating the precise separation and categorization of materials for recycling purposes. This contributes to a reduction in construction waste, a major source of environmental degradation.

The next steps in the project will involve the detailed design of the mobile base and the external frame of the robot. This includes studying the mechanical characteristics of the materials used and developing an initial prototype that functions according to the proposed model. Additionally, a more detailed study of the static and, most importantly, dynamic model will be conducted to understand the limits of speed, acceleration, and overall stability of the robot.

Future work should aim to enhance the robot's adaptability to various environmental conditions and explore the potential for autonomous decision-making based on real-time data analysis. Enhancing these aspects of the robot's functionality could revolutionize the field, making autonomous robotic demolition a standard practice in the industry.

Bibliografia

- [1] Beginner's guide to depth, July 2019. <https://www.intelrealsense.com/beginners-guide-to-depth/>.
- [2] Maximum Axis Speed/Acceleration, 4 2021. <https://forum.universal-robots.com/t/maximum-axis-speed-acceleration/13338/4>.
- [3] Antonio Adán, Blanca Quintana, and Samuel A. Prieto. Autonomous mobile scanning systems for the digitization of buildings: A review. *Remote. Sens.*, 11:306, 2019.
- [4] Joan Badia Torres, Alba Perez Gracia, and Carles Domenech-Mestres. Driving strategies for omnidirectional mobile robots with offset differential wheels. *Robotics*, 13, 2024.
- [5] Andrea Benedetto, Fabio Tosti, Luca Bianchini Ciampoli, and Fabrizio D'Amico. Gpr applications across engineering and geosciences disciplines in italy: A review. *IEEE Journal of Selected Topics in Applied Earth Observations and Remote Sensing*, 9(7):2952–2965, 2016.
- [6] Milan Beres Jr and FP Haeni. Application of ground-penetrating-radar methods in hydrogeologie studies. *Groundwater*, 29(3):375–386, 1991.
- [7] Joydeep Biswas and Manuela Veloso. Depth camera based indoor mobile robot localization and navigation. In *2012 IEEE International Conference on Robotics and Automation*, pages 1697–1702. IEEE, 2012.
- [8] Dengsheng Cai, Zhigang Lu, Xiangsuo Fan, Jiale Yao, and Bing Li. Material identification of construction machinery based on multisource sensor information fusion. *Engineering Reports*, 4, 03 2022.
- [9] J.; Domènech Canuto Gil. Patent: Omnidirectional platform and omnidirectional conveyor. *U.S. Patent WO2019020861A2*, 17 May 2018.
- [10] Jeffrey Daniels. Ground penetrating radar fundamentals. 01 2000.
- [11] Ministerio das Obras Públicas Gabinete do Ministro. Decreto-lei n.º 38382. *Diário do Governo n.º 166/1951, 1º Suplemento, Série I de 1951-08-07, páginas 715 - 729*, 1951.
- [12] Rory Daulton. moving pipe around corner. <https://math.stackexchange.com/questions/1554503/moving-pipe-around-corner>, Accessed July 12,2024.
- [13] Ministerio de la Vivienda. Normas de diseño y calidad de las viviendas sociales. «BOE»

núm. 141, de 14 de junio de 1977, páginas 13305 a 13329, 1977.

- [14] Agencia Estatal Boletín Oficial del Estado. Boe-a-1969-622. «BOE» núm. 123, de 23 de mayo de 1969, páginas 7918 a 7923, 1969.
- [15] Heiko Engemann, Shengzhi Du, Stephan Kallweit, Patrick Cönen, and Harshal Dawar. Omnivil—an autonomous mobile manipulator for flexible production. *Sensors*, 20(24), 2020.
- [16] Carlotta Ferrara and Pier Matteo Barone. Detecting moisture damage in archaeology and cultural heritage sites using the gpr technique: A brief introduction. *Int. J. Archaeol*, 3(1-1):57–61, 2015.
- [17] Usha Iyer-Raniga. Zero energy in the built environment: A holistic understanding. *Applied Sciences*, 9(16):3375, 2019.
- [18] Seongki Lee, Wen Pan, Thomas Linner, and Thomas Bock. A framework for robot assisted deconstruction: Process, sub-systems and modelling. 2015.
- [19] Nanxi Li, Chong Pei Ho, Jin Xue, Leh Woon Lim, Guanyu Chen, Yuan Hsing Fu, and Lennon Yao Ting Lee. A progress review on solid-state lidar and nanophotonics-based lidar sensors. *Laser & Photonics Reviews*, 16(11):2100511, 2022.
- [20] Daniel Maier, Armin Hornung, and Maren Bennewitz. Real-time navigation in 3d environments based on depth camera data. In *2012 12th IEEE-RAS International Conference on Humanoid Robots (Humanoids 2012)*, pages 692–697. IEEE, 2012.
- [21] Ninad Mehendale and Srushti Neoge. Review on lidar technology. *Available at SSRN 3604309*, 2020.
- [22] João Pedro, Frits Meijer, and Henk Visscher. The portuguese building regulation system: A critical review. *International Journal of Law in the Built Environment*, 1:156–171, 07 2009.
- [23] Jae-Bok Song and Kyung-Seok Byun. Design and control of an omnidirectional mobile robot with steerable omnidirectional wheels. In *Mobile Robotics, Moving Intelligence*. IntechOpen, 2006.
- [24] Zheng Tong, Jie Gao, and Dongdong Yuan. Advances of deep learning applications in ground-penetrating radar: A survey. *Construction and Building Materials*, 258:120371, 2020.

- [25] Ulrich Weiss and Peter Biber. Plant detection and mapping for agricultural robots using a 3d lidar sensor. *Robotics and autonomous systems*, 59(5):265–273, 2011.
- [26] Xiaoping Yun and Yoshio Yamamoto. Stability analysis of the internal dynamics of a wheeled mobile robot. *Journal of Robotic Systems*, 14(10):697–709, 1997.
- [27] Wael Zatar, Tu T. Nguyen, and Hai Nguyen. Predicting gpr signals from concrete structures using artificial intelligence-based method. *Advances in Civil Engineering*, 2021:1–9, 02 2021.

Ringraziamenti

Vorrei spendere due parole per tutte le persone che mi hanno accompagnato in questi anni.

Grazie ai miei genitori che mi hanno permesso di studiare supportandomi sempre e comunque, ma soprattutto grazie per tutto l'amore che mi avete donato.

Grazie a mio fratello Matteo per essermi sempre stato vicino, anche nella distanza e nel silenzio.

Grazie a nonna Gemma che mi pensa sempre e farebbe di tutto per me.

Graie ai nonni che non sono più tra noi, ma per sempre nel mio cuore.

Grazie a tutta la famiglia che mi ha sempre dimostrato affetto e con cui ho la fortuna di condividere i momenti di festa.

Grazie agli amici che non mi hanno mai lasciato solo e con cui condivido ricordi preziosi.

Grazie a chi mi vuole bene, a chi lo ha fatto e a chi lo farà.

*Con enorme affetto,
Francesco*